



IJOER
RESEARCH JOURNAL

ISSN

2395-6992

International Journal of Engineering Research & Science

www.ijoer.com

www.adpublications.org

Volume-8! Issue-10! October, 2022

www.ijoer.com ! info@ijoer.com

Preface

We would like to present, with great pleasure, the inaugural volume-8, Issue-10, October 2022, of a scholarly journal, *International Journal of Engineering Research & Science*. This journal is part of the AD Publications series *in the field of Engineering, Mathematics, Physics, Chemistry and science Research Development*, and is devoted to the gamut of Engineering and Science issues, from theoretical aspects to application-dependent studies and the validation of emerging technologies.

This journal was envisioned and founded to represent the growing needs of Engineering and Science as an emerging and increasingly vital field, now widely recognized as an integral part of scientific and technical investigations. Its mission is to become a voice of the Engineering and Science community, addressing researchers and practitioners in below areas

Chemical Engineering	
Biomolecular Engineering	Materials Engineering
Molecular Engineering	Process Engineering
Corrosion Engineering	
Civil Engineering	
Environmental Engineering	Geotechnical Engineering
Structural Engineering	Mining Engineering
Transport Engineering	Water resources Engineering
Electrical Engineering	
Power System Engineering	Optical Engineering
Mechanical Engineering	
Acoustical Engineering	Manufacturing Engineering
Optomechanical Engineering	Thermal Engineering
Power plant Engineering	Energy Engineering
Sports Engineering	Vehicle Engineering
Software Engineering	
Computer-aided Engineering	Cryptographic Engineering
Teletraffic Engineering	Web Engineering
System Engineering	
Mathematics	
Arithmetic	Algebra
Number theory	Field theory and polynomials
Analysis	Combinatorics
Geometry and topology	Topology
Probability and Statistics	Computational Science
Physical Science	Operational Research
Physics	
Nuclear and particle physics	Atomic, molecular, and optical physics
Condensed matter physics	Astrophysics
Applied Physics	Modern physics
Philosophy	Core theories

Chemistry	
Analytical chemistry	Biochemistry
Inorganic chemistry	Materials chemistry
Neurochemistry	Nuclear chemistry
Organic chemistry	Physical chemistry
Other Engineering Areas	
Aerospace Engineering	Agricultural Engineering
Applied Engineering	Biomedical Engineering
Biological Engineering	Building services Engineering
Energy Engineering	Railway Engineering
Industrial Engineering	Mechatronics Engineering
Management Engineering	Military Engineering
Petroleum Engineering	Nuclear Engineering
Textile Engineering	Nano Engineering
Algorithm and Computational Complexity	Artificial Intelligence
Electronics & Communication Engineering	Image Processing
Information Retrieval	Low Power VLSI Design
Neural Networks	Plastic Engineering

Each article in this issue provides an example of a concrete industrial application or a case study of the presented methodology to amplify the impact of the contribution. We are very thankful to everybody within that community who supported the idea of creating a new Research with IJOER. We are certain that this issue will be followed by many others, reporting new developments in the Engineering and Science field. This issue would not have been possible without the great support of the Reviewer, Editorial Board members and also with our Advisory Board Members, and we would like to express our sincere thanks to all of them. We would also like to express our gratitude to the editorial staff of AD Publications, who supported us at every stage of the project. It is our hope that this fine collection of articles will be a valuable resource for *IJOER* readers and will stimulate further research into the vibrant area of Engineering and Science Research.



Mukesh Arora
(Chief Editor)

Board Members

Mr. Mukesh Arora (Editor-in-Chief)

BE (Electronics & Communication), M.Tech (Digital Communication), currently serving as Assistant Professor in the Department of ECE.

Prof. Dr. Fabricio Moraes de Almeida

Professor of Doctoral and Master of Regional Development and Environment - Federal University of Rondonia.

Dr. Parveen Sharma

Dr Parveen Sharma is working as an Assistant Professor in the School of Mechanical Engineering at Lovely Professional University, Phagwara, Punjab.

Prof. S. Balamurugan

Department of Information Technology, Kalaingar Karunanidhi Institute of Technology, Coimbatore, Tamilnadu, India.

Dr. Omar Abed Elkareem Abu Arqub

Department of Mathematics, Faculty of Science, Al Balqa Applied University, Salt Campus, Salt, Jordan, He received PhD and Msc. in Applied Mathematics, The University of Jordan, Jordan.

Dr. AKPOJARO Jackson

Associate Professor/HOD, Department of Mathematical and Physical Sciences, Samuel Adegboyega University, Ogwa, Edo State.

Dr. Ajoy Chakraborty

Ph.D.(IIT Kharagpur) working as Professor in the department of Electronics & Electrical Communication Engineering in IIT Kharagpur since 1977.

Dr. Ukar W. Soelistijo

Ph D, Mineral and Energy Resource Economics, West Virginia State University, USA, 1984, retired from the post of Senior Researcher, Mineral and Coal Technology R&D Center, Agency for Energy and Mineral Research, Ministry of Energy and Mineral Resources, Indonesia.

Dr. Samy Khalaf Allah Ibrahim

PhD of Irrigation &Hydraulics Engineering, 01/2012 under the title of: "Groundwater Management under Different Development Plans in Farafra Oasis, Western Desert, Egypt".

Dr. Ahmet ÇİFCİ

Ph.D. in Electrical Engineering, Currently Serving as Head of Department, Burdur Mehmet Akif Ersoy University, Faculty of Engineering and Architecture, Department of Electrical Engineering.

Dr. M. Varatha Vijayan

Annauniversity Rank Holder, Commissioned Officer Indian Navy, Ncc Navy Officer (Ex-Serviceman Navy), Best Researcher Awardee, Best Publication Awardee, Tamilnadu Best Innovation & Social Service Awardee From Lions Club.

Dr. Mohamed Abdel Fatah Ashabrawy Moustafa

PhD. in Computer Science - Faculty of Science - Suez Canal University University, 2010, Egypt.

Assistant Professor Computer Science, Prince Sattam bin AbdulAziz University ALkharj, KSA.

Prof.S.Balamurugan

Dr S. Balamurugan is the Head of Research and Development, Quants IS & CS, India. He has authored/co-authored 35 books, 200+ publications in various international journals and conferences and 6 patents to his credit. He was awarded with Three Post-Doctoral Degrees - Doctor of Science (D.Sc.) degree and Two Doctor of Letters (D.Litt) degrees for his significant contribution to research and development in Engineering.

Dr. Mahdi Hosseini

Dr. Mahdi did his Pre-University (12th) in Mathematical Science. Later he received his Bachelor of Engineering with Distinction in Civil Engineering and later he Received both M.Tech. and Ph.D. Degree in Structural Engineering with Grade "A" First Class with Distinction.

Dr. Anil Lamba

Practice Head – Cyber Security, EXL Services Inc., New Jersey USA.

Dr. Anil Lamba is a researcher, an innovator, and an influencer with proven success in spearheading Strategic Information Security Initiatives and Large-scale IT Infrastructure projects across industry verticals. He has helped bring about a profound shift in cybersecurity defense. Throughout his career, he has parlayed his extensive background in security and a deep knowledge to help organizations build and implement strategic cybersecurity solutions. His published researches and conference papers has led to many thought provoking examples for augmenting better security.

Dr. Ali İhsan KAYA

Currently working as Associate Professor in Mehmet Akif Ersoy University, Turkey.

Research Area: Civil Engineering - Building Material - Insulation Materials Applications, Chemistry - Physical Chemistry – Composites.

Dr. Parsa Heydarpour

Ph.D. in Structural Engineering from George Washington University (Jan 2018), GPA=4.00.

Dr. Heba Mahmoud Mohamed Afify

Ph.D degree of philosophy in Biomedical Engineering, Cairo University, Egypt worked as Assistant Professor at MTI University.

Dr. Aurora Angela Pisano

Ph.D. in Civil Engineering, Currently Serving as Associate Professor of Solid and Structural Mechanics (scientific discipline area nationally denoted as ICAR/08—"Scienza delle Costruzioni"), University Mediterranea of Reggio Calabria, Italy.

Dr. Faizullah Mahar

Associate Professor in Department of Electrical Engineering, Balochistan University Engineering & Technology Khuzdar. He is PhD (Electronic Engineering) from IQRA University, Defense View, Karachi, Pakistan.

Prof. Viviane Barrozo da Silva

Graduated in Physics from the Federal University of Paraná (1997), graduated in Electrical Engineering from the Federal University of Rio Grande do Sul - UFRGS (2008), and master's degree in Physics from the Federal University of Rio Grande do Sul (2001).

Dr. S. Kannadhasan

Ph.D (Smart Antennas), M.E (Communication Systems), M.B.A (Human Resources).

Dr. Christo Ananth

Ph.D. Co-operative Networks, M.E. Applied Electronics, B.E Electronics & Communication Engineering Working as Associate Professor, Lecturer and Faculty Advisor/ Department of Electronics & Communication Engineering in Francis Xavier Engineering College, Tirunelveli.

Dr. S.R.Boselin Prabhu

Ph.D, Wireless Sensor Networks, M.E. Network Engineering, Excellent Professional Achievement Award Winner from Society of Professional Engineers Biography Included in Marquis Who's Who in the World (Academic Year 2015 and 2016). Currently Serving as Assistant Professor in the department of ECE in SVS College of Engineering, Coimbatore.

Dr. PAUL P MATHAI

Dr. Paul P Mathai received his Bachelor's degree in Computer Science and Engineering from University of Madras, India. Then he obtained his Master's degree in Computer and Information Technology from Manonmanium Sundaranar University, India. In 2018, he received his Doctor of Philosophy in Computer Science and Engineering from Noorul Islam Centre for Higher Education, Kanyakumari, India.

Dr. M. Ramesh Kumar

Ph.D (Computer Science and Engineering), M.E (Computer Science and Engineering).

Currently working as Associate Professor in VSB College of Engineering Technical Campus, Coimbatore.

Dr. Maheshwar Shrestha

Postdoctoral Research Fellow in DEPT. OF ELE ENGG & COMP SCI, SDSU, Brookings, SD Ph.D, M.Sc. in Electrical Engineering from SOUTH DAKOTA STATE UNIVERSITY, Brookings, SD.

Dr. D. Amaranatha Reddy

Ph.D. (Postdoctoral Fellow, Pusan National University, South Korea), M.Sc., B.Sc. : Physics.

Dr. Dibya Prakash Rai

Post Doctoral Fellow (PDF), M.Sc., B.Sc., Working as Assistant Professor in Department of Physics in Pachhungga University College, Mizoram, India.

Dr. Pankaj Kumar Pal

Ph.D R/S, ECE Deptt., IIT-Roorkee.

Dr. P. Thangam

PhD in Information & Communication Engineering, ME (CSE), BE (Computer Hardware & Software), currently serving as Associate Professor in the Department of Computer Science and Engineering of Coimbatore Institute of Engineering and Technology.

Dr. Pradeep K. Sharma

PhD., M.Phil, M.Sc, B.Sc, in Physics, MBA in System Management, Presently working as Provost and Associate Professor & Head of Department for Physics in University of Engineering & Management, Jaipur.

Dr. R. Devi Priya

Ph.D (CSE), Anna University Chennai in 2013, M.E, B.E (CSE) from Kongu Engineering College, currently working in the Department of Computer Science and Engineering in Kongu Engineering College, Tamil Nadu, India.

Dr. Sandeep

Post-doctoral fellow, Principal Investigator, Young Scientist Scheme Project (DST-SERB), Department of Physics, Mizoram University, Aizawl Mizoram, India- 796001.

Dr. Roberto Volpe

Faculty of Engineering and Architecture, Università degli Studi di Enna "Kore", Cittadella Universitaria, 94100 – Enna (IT).

Dr. S. Kannadhasan

Ph.D (Smart Antennas), M.E (Communication Systems), M.B.A (Human Resources).

Research Area: Engineering Physics, Electromagnetic Field Theory, Electronic Material and Processes, Wireless Communications.

Mr. Amit Kumar

Amit Kumar is associated as a Researcher with the Department of Computer Science, College of Information Science and Technology, Nanjing Forestry University, Nanjing, China since 2009. He is working as a State Representative (HP), Spoken Tutorial Project, IIT Bombay promoting and integrating ICT in Literacy through Free and Open Source Software under National Mission on Education through ICT (NMEICT) of MHRD, Govt. of India; in the state of Himachal Pradesh, India.

Mr. Tanvir Singh

Tanvir Singh is acting as Outreach Officer (Punjab and J&K) for MHRD Govt. of India Project: Spoken Tutorial - IIT Bombay fostering IT Literacy through Open Source Technology under National Mission on Education through ICT (NMEICT). He is also acting as Research Associate since 2010 with Nanjing Forestry University, Nanjing, Jiangsu, China in the field of Social and Environmental Sustainability.

Mr. Abilash

M.Tech in VLSI, BTech in Electronics & Telecommunication engineering through A.M.I.E.T.E from Central Electronics Engineering Research Institute (C.E.E.R.I) Pilani, Industrial Electronics from ATI-EPI Hyderabad, IEEE course in Mechatronics, CSHAM from Birla Institute Of Professional Studies.

Mr. Varun Shukla

M.Tech in ECE from RGPV (Awarded with silver Medal By President of India), Assistant Professor, Dept. of ECE, PSIT, Kanpur.

Mr. Shrikant Harle

Presently working as a Assistant Professor in Civil Engineering field of Prof. Ram Meghe College of Engineering and Management, Amravati. He was Senior Design Engineer (Larsen & Toubro Limited, India).

Zairi Ismael Rizman

Senior Lecturer, Faculty of Electrical Engineering, Universiti Teknologi MARA (UiTM) (Terengganu) Malaysia Master (Science) in Microelectronics (2005), Universiti Kebangsaan Malaysia (UKM), Malaysia. Bachelor (Hons.) and Diploma in Electrical Engineering (Communication) (2002), UiTM Shah Alam, Malaysia.

Mr. Ronak

Qualification: M.Tech. in Mechanical Engineering (CAD/CAM), B.E.

Presently working as a Assistant Professor in Mechanical Engineering in ITM Vocational University, Vadodara. Mr. Ronak also worked as Design Engineer at Finstern Engineering Private Limited, Makarpura, Vadodara.

Table of Contents

Volume-8, Issue-10, October 2022

S. No	Title	Page No.
1	Effect Of Heating Rate and Sintering Temperature on Mechanical Properties of W-Cu Composites Produced via Spark Plasma Sintering Authors: Nguyen Minh Tuan, Nguyen Ngoc Linh, Nguyen Van Toan  DOI: https://dx.doi.org/10.5281/zenodo.7265932  Digital Identification Number: IJOER-OCT-2022-1	01-06
2	Design of the Two-Wheeled Vehicle using Metal Hydride Vessels Authors: Filip Duda, Natalia Jasminska, Ivan Mihalik, Romana Dobakova  DOI: https://dx.doi.org/10.5281/zenodo.7265934  Digital Identification Number: IJOER-OCT-2022-2	07-12
3	Suitability of using Silica Gel in Powder Form as an Adsorbent in the Drying Process Authors: Romana Dobakova, Filip Duda, Ivan Mihalik, Tomas Brestovic  DOI: https://dx.doi.org/10.5281/zenodo.7265940  Digital Identification Number: IJOER-OCT-2022-3	13-17
4	Yeast Strains from <i>Burukutu</i> and <i>Fura</i>, as an Alternative for Commercial Baker's Yeast Authors: Umeh, S.O.; Igwilo, I.O.; Okafor, U.C.; Agbara, A.C; Ezeh F. N.  DOI: https://dx.doi.org/10.5281/zenodo.7265942  Digital Identification Number: IJOER-OCT-2022-4	18-23
5	Indoor Environment of Buildings – Quality and Basic Ventilation Air Parameters: Part I Authors: Lubomira Kmetova, Romana Dobakova, Lukas Toth  DOI: https://dx.doi.org/10.5281/zenodo.7265947  Digital Identification Number: IJOER-OCT-2022-5	24-28
6	Comparison of Different Natural Gas Flow Rates in Pipelines and their Effect on Odorant Concentration Authors: Ivan Mihalik, Tomas Brestovic, Romana Dobakova, Lukas Toth  DOI: https://dx.doi.org/10.5281/zenodo.7265953  Digital Identification Number: IJOER-OCT-2022-6	29-34

Effect Of Heating Rate and Sintering Temperature on Mechanical Properties of W-Cu Composites Produced via Spark Plasma Sintering

Nguyen Minh Tuan¹, Nguyen Ngoc Linh², Nguyen Van Toan³

¹Graduate University of Science and Technology, VietNam Academy of Science and Technology, No.18 Hoang Quoc Viet Str., Cau Giay Distr., Hanoi, Vietnam

^{2,3}Institute of Materials Science, Vietnam Academy of Science and Technology, No.18 Hoang Quoc Viet Str., Cau Giay Distr., Hanoi, Vietnam

*Corresponding Author

Received: 29 September 2022/ Revised: 11 October 2022/ Accepted: 17 October 2022/ Published: 31-10-2022
Copyright @ 2021 International Journal of Engineering Research and Science

This is an Open-Access article distributed under the terms of the Creative Commons Attribution Non-Commercial License (<https://creativecommons.org/licenses/by-nc/4.0>) which permits unrestricted Non-commercial use, distribution, and reproduction in any medium, provided the original work is properly cited.

Abstract— This work was done to investigate the effect of heating rate and sintering temperature on the structure and mechanical properties of W-50Cu (wt.%) composites using spark plasma sintering technique. For investigate the effect of sintering temperature, the W-50Cu composites were sintered at temperature in the range of 900 to 975°C for 30 min using the heating rate of 50 °C/min meanwhile in order to see the effect of heating rate, the composites were sintered at 950 °C for 30 min at different heating rate from 25 to 200°C/min. The results show that all the sintered composites have a good distribution of W particles in Cu matrix. The increase of sintering temperature led to higher density, larger W average particle size and better strain at break (by compressive test), however, the hardness has a tendency to decrease at higher sintering temperature. The heating rate how an opposite effect in comparison with sintered temperature. The increase of heating rate led to the lower density, smaller W particles and lower strain at break of sintered sample but higher Vickers hardness.

Keywords— W-50Cu composites, heating rate, strain at break.

I. INTRODUCTION

Tungsten-copper (W-Cu) based composites have been attracted in many fields due to their high hardness and wear resistance, good electrical conductivity as well as the low coefficients of thermal expansion and good electric-erosion resistance [1, 2]. The applications of these composites are the electric and electronic materials for resistance welding electrodes, electric discharge machine, heat-sink materials and potential materials for military applications including armor-piercing, shaped charge liner and ammunition materials [1, 3-6]. Because of the large deviation in melting point between W and Cu, W-Cu based composites are fabricated by powder metallurgy technology including liquid phase sintering and infiltration [7-9]. The infiltration is commonly used method in which a porous-sintered tungsten skeleton is filled with melted copper. However, in this technique, the pores, copper pools and also the agglomeration of tungsten are easily formed [8]. These defects lead to the degradation of the W-Cu composite's properties. Liquid phase sintering (LPS) is the next popular method to produce W-Cu composites. This technique consists of three steps; mixing W and Cu powders by mechanical milling, compressing the mixture powders and follows by sintering at the temperature higher than melting point of Cu [1, 2]. But, liquid phase sintering may result in the coarse grain growth of W during sintering and it is difficult to obtain the full density of the specimens because of the poor solubility and wettability between W and Cu. Therefore, advanced methods have been applied to enhance the properties of W-Cu composites such as microwave sintering [10, 11], hot extrusion [12], powder injection molding [13] or

spark plasma sintering (SPS) [1, 2, 9, 14, 15], etc. SPS is an advanced technique in which the samples are quickly heated to the sintering temperature with a controlled pressure at the same time. The high heating rate and the application of pressure during sintering lead to a better contact between particles and an improvement of the sample densification in a very short time [16]. In addition, SPS is a candidate method to consolidate the W-Cu composites with controllable structure, good densification and energy saving [14]. This research was carried out to investigate the effect of the sintering temperature and heating rate on the structure, density and mechanical properties of W-50Cu composites produced by SPS method.

II. EXPERIMENTAL

In this work, W-50Cu (wt.%) composites were consolidated by SPS at different sintering temperatures and heating rate. W and Cu powders had a purity of 99.9 % (particle size in the range of 44-75 μm for both W and Cu powders). The mixture powders were ball milled for 48 hours in n-hexane medium using ball-to-powder ratio of 2:1. The balls and jar were made of WC-Co hard alloys. After milling, the mixture powders were hydrothermal treatment at 300 $^{\circ}\text{C}$ for 1 hour to eliminate the Cu oxide presented in the mixture powders. After pre-compaction at the pressure of 100 MPa, the pellet samples were pre-heated at 900 $^{\circ}\text{C}$ for 1 hour in hydrogen gas flow. The SPS process was done on Labox 350 system (Sinterland, Japan) using graphite mold with 10 mm in diameter under vacuum level at 6 Pa. To investigate the effect of sintering temperature, the pellets were sintered at 900, 925, 950 and 975 $^{\circ}\text{C}$ for 30 min using the heating rate of 50 $^{\circ}\text{C}/\text{min}$. In order to study the effect of heating rate, the pellets were sintered at 950 $^{\circ}\text{C}$ for 30 min using the heating rate of 25, 50, 75, 100 and 200 $^{\circ}\text{C}/\text{min}$. The phase component of specimens was investigated on the X-rays diffractometer ($\text{K}\alpha\text{-Cu}$: 1.5406 \AA , XRD D8, ADVANCE Bruker) whirled the microstructure of samples was observed on a Field emission scanning electron microscopy (FE-SEM, Hitachi S4800). The density was measured based on Archimedes's principle (AND GN202, Japan). Vickers hardness was tested at the load of 5 Kg and the dwelling time of 10 s (Mitutiyo AVK-C0). For compression test, the samples were cut in the cylindrical shape with the height of 6 mm and a diameter of 4 mm. The compression test was carried out on the Super L120 equipment (Tinius Olsen) using a strain rate of $10^{-3} \cdot \text{s}^{-1}$.

III. RESULTS AND DISCUSSION

3.1 Effect of the sintering temperature

Fig. 1 shows the SEM images and the W particle size distribution of W-50Cu composites at different sintered temperatures. The SEM images demonstrate the homogenous distribution of W particles in the Cu matrix for all sintered temperatures. It is obvious that the increase of sintering temperature leads to the increase of W particle size. The average particle size calculations are 19.2, 20.5, 22.7 and 24.8 μm corresponding to the sintering temperature of 900, 925, 950 and 975 $^{\circ}\text{C}$, respectively. As the rising of sintered temperature, the thermal dynamic of sintered process and grain growth were improved, and W particles have a trend to merge with their neighbor particles to become larger particles and with more round shapes. In addition, the pores would be eliminated toward the rising of the sintering temperature. The density of sintered samples and Vickers hardness are plotted as seen in Fig. 2a. The density increased from 11.60 to 12.05 g/cm^3 corresponding the sintering temperature from 900 to 975 $^{\circ}\text{C}$. The higher sintering temperature improved the sintering characteristic of the composites. The Vickers hardness the specimens is enhanced from 147 to 156 HV5 when the sintered temperature increased from 900 to 950 $^{\circ}\text{C}$, however, the hardness was then dropped to 143 HV5 at the sintering temperature of 975 $^{\circ}\text{C}$ which could be due to the growth of both W and Cu grains at high sintering temperature. Fig. 2b presents the stress – strain curves meanwhile Fig. 3 shows the effect of sintering temperature on the yield strength, ultimate strength and strain at break of sintered samples. The highest ultimate strength is reached at 892 MPa for the sample sintered at 925 $^{\circ}\text{C}$, however, the values of yield strength and strains at break are lower. Increase the sintering temperature to 950 and 975 $^{\circ}\text{C}$ improves both yield strength and strain at break although the ultimate strength has a trend to decrease, slightly.

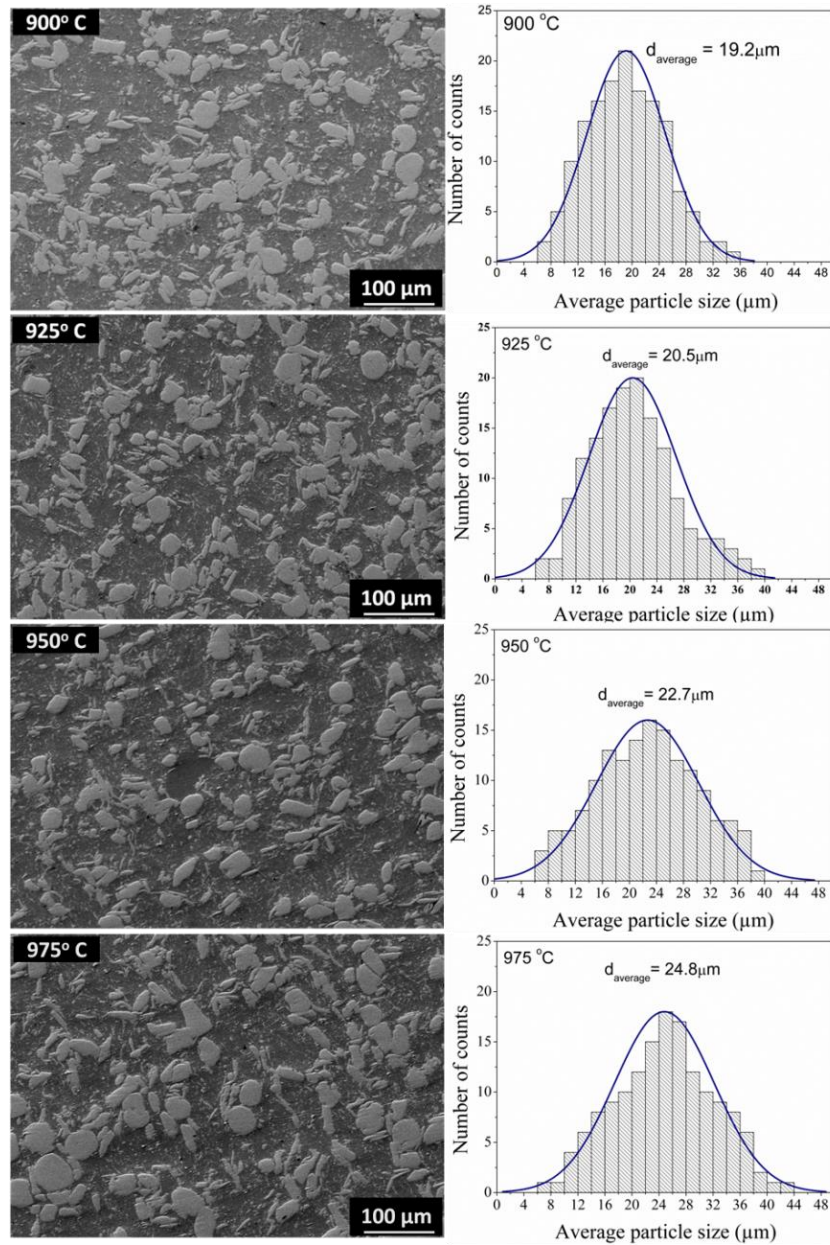


FIGURE 1: SEM images and particle size distribution of samples at different sintered temperatures

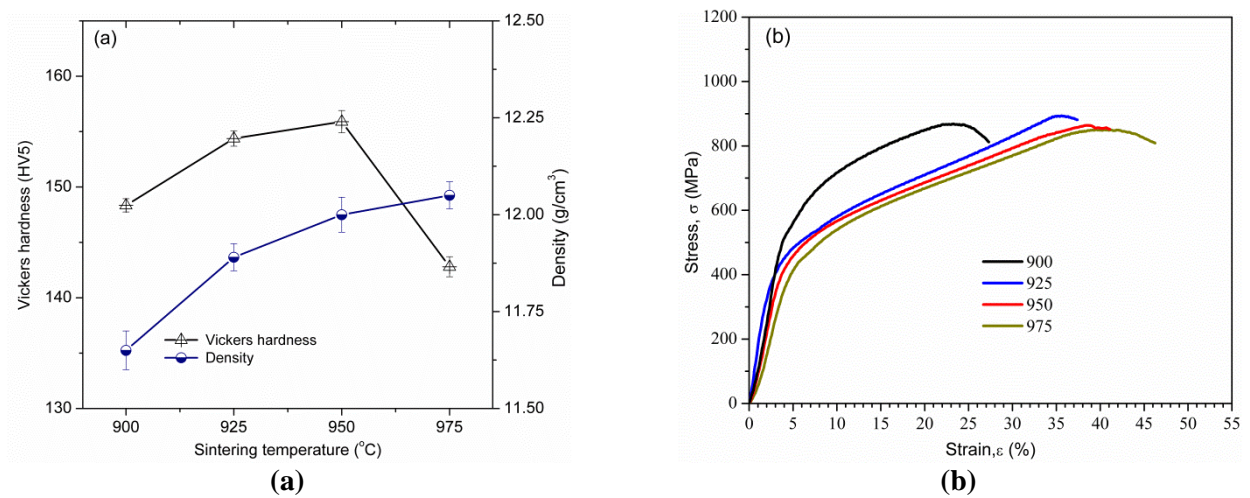


FIGURE 2. a) Density and Vickers hardness, and b) Stress – strain curves of samples at different sintered temperatures

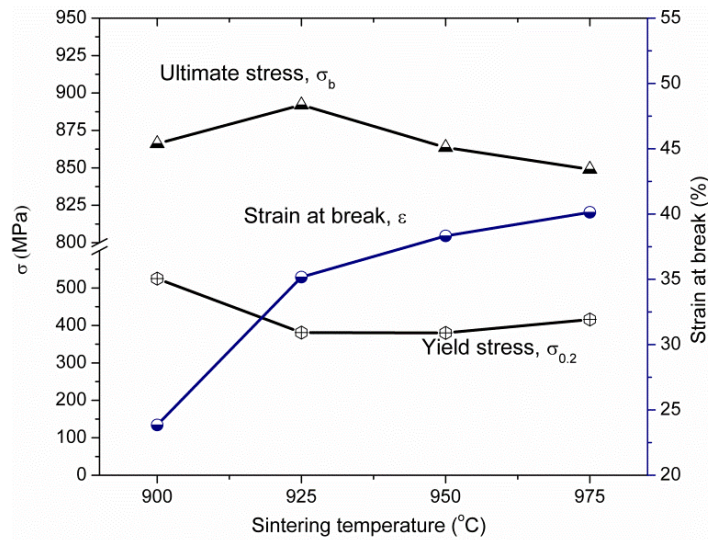


FIGURE 3: Ultimate strength, yield strength and strain at break verify with sintering temperature

3.2 Effect of the heating rate

Fig. 4 shows the SEM images of samples sintered at 950 °C for different heating rates in the range of 25 to 200 °C/min. The good particle distribution of W particles in Cu matrix could be seen. Although the samples were sintered at the same temperature, SEM images also show the larger particle size observed for lower heating rate due to the longer of the total sintering time. The particle size distribution of all samples are presented in Fig. 5 which demonstrated the particle size distribution spectra shifted to the smaller size of particles with the increase of the heating rate. Nevertheless, the high heating rate led to faster welding of Cu particles resulting in the inhibition of pore movement out of the bulk. So, the residual pores still presented in the samples which evidenced by the reduction of the density of sintered samples when the heating rate increased, as shown in Fig. 6a. Fig. 6a also show an improvement of hardness with the heating rate which could be attributed to the reduction of WC particle size due to the increase of the heating rate. Fig. 6b shows the compressive stress-strain curves of sintered samples while Fig. 7 reveals the effect of the heating rate on yield stress, ultimate stress and strain at break of all specimens. As shown in Fig. 7, the yield strength is enhanced with the increase of heating rate and reached the highest value at 472 MPa for the sample sintered at the heating rate of 200 °C/min while strain at break has a trend to decrease from 40.9 to 20.4 % as the heating rate rising from 25 to 200 °C/min. The reduction of strain at break may be due to the residual pores at higher heating rates. The ultimate stress, however, presents a fluctuation in their values and obtained the peak at 847 MPa for the heating rate of 50 °C/min.

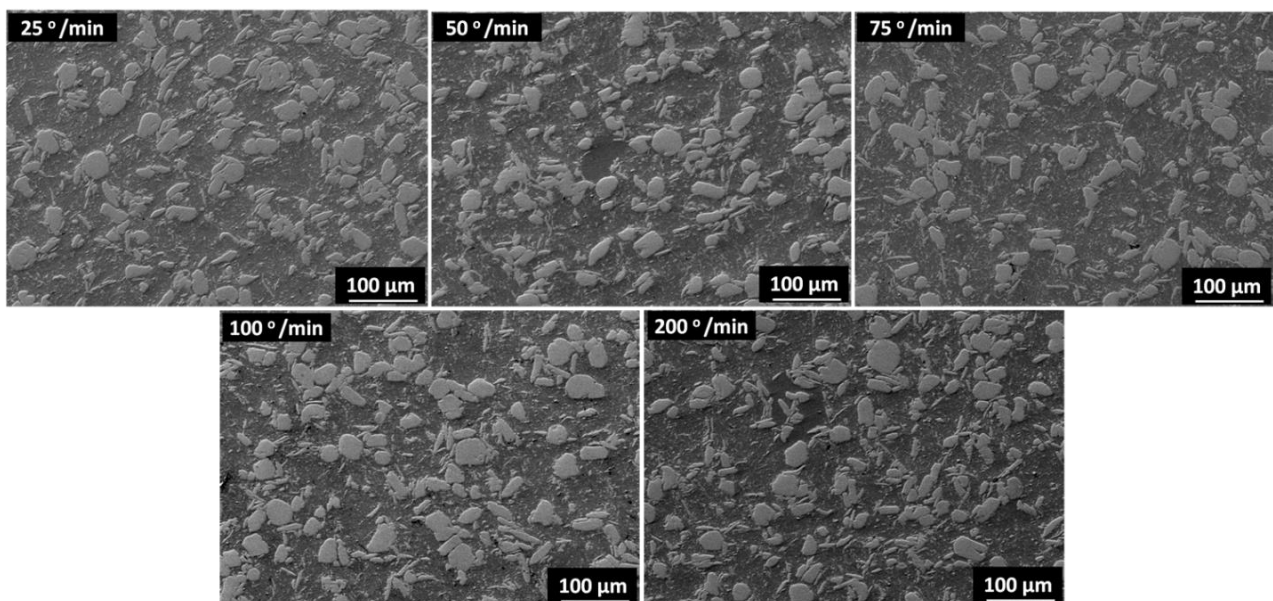


FIGURE 4: SEM images of W-Cu composites sintered at different heating rates

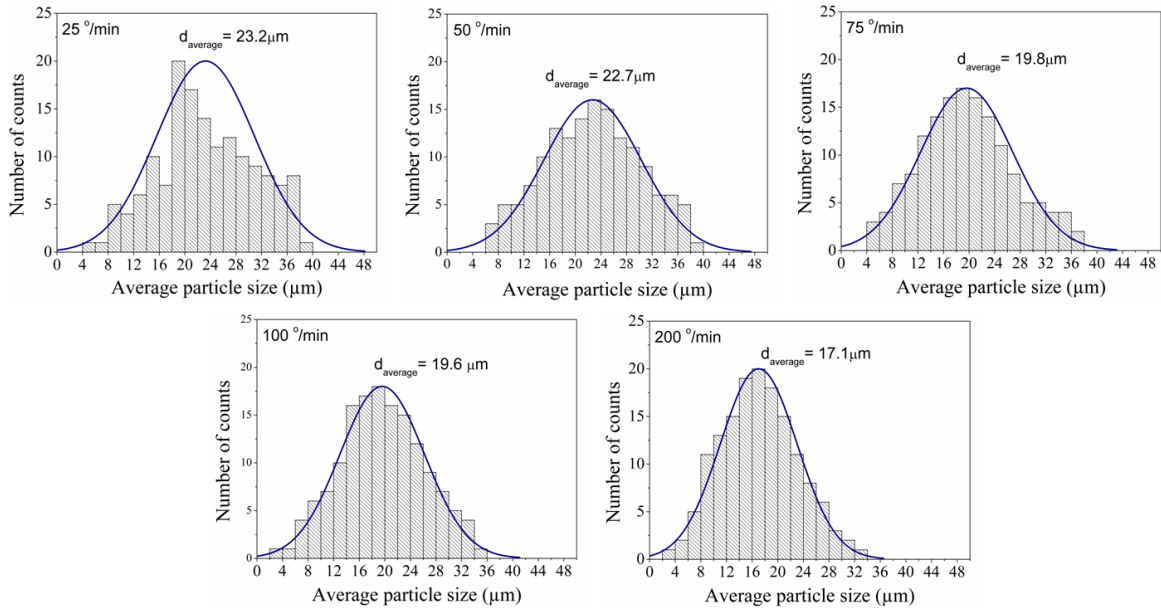


FIGURE 5: Effect of the heating rate on W particle size distribution on Cu matrix

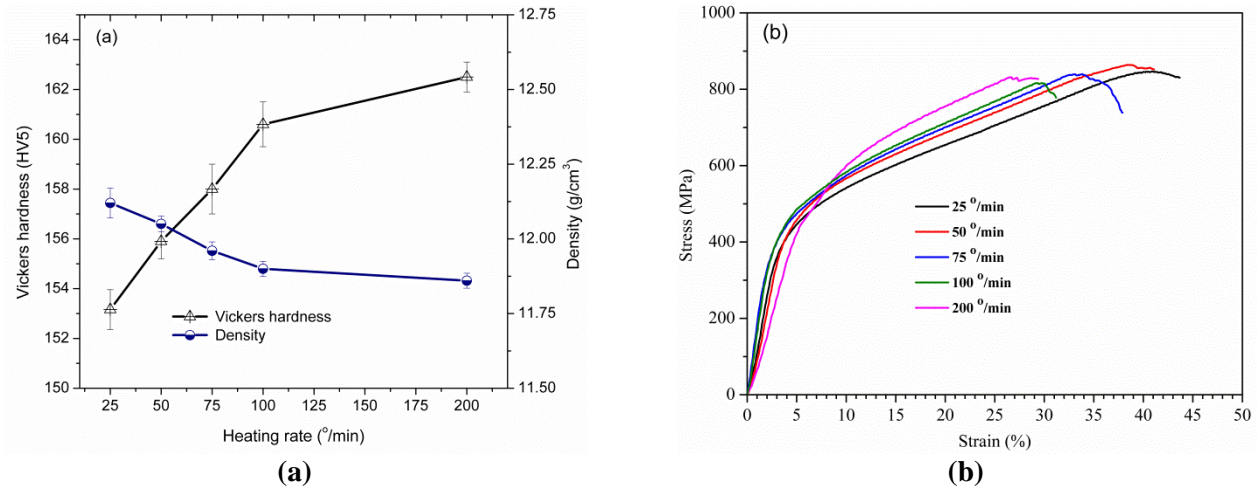


FIGURE 6: a) Density and Vickers hardness, and b) Stress – strain curves of samples at different heating rate

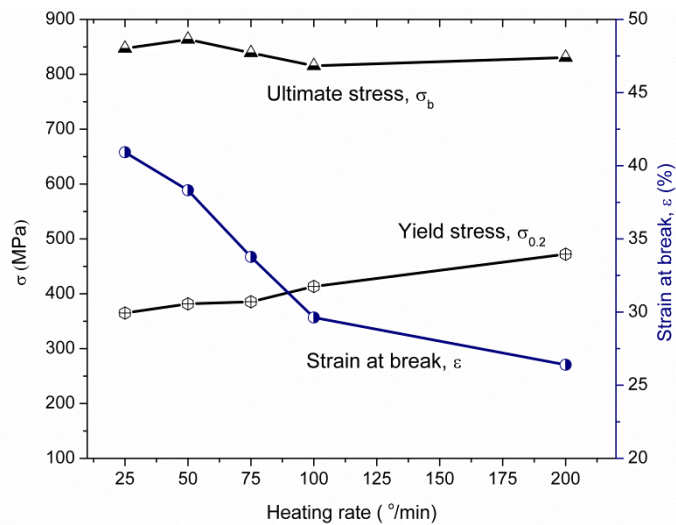


FIGURE 7: Ultimate strength, yield strength and strain at break verify with the heating rate

IV. CONCLUSION

In this work, W-50Cu composites have been produced by powder route using spark plasma sintering technique. The effect of the sintering temperature and heating rate on the structure and mechanical properties of the sintered has been investigated. The conclusions are as following:

The increase of sintering temperature led to the higher density, larger W particles and resulted in the better strain at break of sintered samples. The Vickers hardness has been improved with the rising temperature from 900 to 950 °C, but further increase of sintering temperature caused the reduction of Vickers hardness.

On the contrary, the faster heating rate led to the reduction of density and smaller average W particle size. In addition, the higher heating rate also led to more residual pores in the W-50Cu structure and therefore, lowers the strain at break of sintered sample. The Vickers hardness shows an increase with heating rate. This could be due to the smaller average particle size of W particles in Cu matrix.

REFERENCES

- [1] Dong, L.L., et al., Recent progress in development of tungsten-copper composites: Fabrication, modification and applications. *International Journal of Refractory Metals and Hard Materials*, 2018. 75: p. 30-42.
- [2] Hou, C., et al., W–Cu composites with submicron- and nanostructures: progress and challenges. *NPG Asia Materials*, 2019. 11(1): p. 74.
- [3] Chen, Q., et al., Microstructural investigation after vacuum electrical breakdown of the W-30wt.%Cu contact material. *Vacuum*, 2018. 149: p. 256-261.
- [4] Zhuo, L., et al., Achieving both high conductivity and reliable high strength for W–Cu composite alloys using spherical initial powders. *Vacuum*, 2020. 181: p. 109620.
- [5] Roosta, M., H. Baharvandi, and H. Abdizade, An experimental investigation on the fabrication of W-Cu composite through hot-press. *International Journal of Industrial Chemistry*, 2012. 3(1): p. 10.
- [6] Zhao, Z., et al., Effect of Zn and Ni added in W–Cu alloy on penetration performance and penetration mechanism of shaped charge liner. *International Journal of Refractory Metals and Hard Materials*, 2016. 54: p. 90-97.
- [7] Ibrahim, H., A. Aziz, and A. Rahmat, Enhanced liquid-phase sintering of W–Cu composites by liquid infiltration. *International Journal of Refractory Metals and Hard Materials*, 2014. 43: p. 222-226.
- [8] Liu, J.-K., et al., Fabrication of ultrafine W-Cu composite powders and its sintering behavior. *Journal of Materials Research and Technology*, 2020. 9(2): p. 2154-2163.
- [9] Zhou, K., et al., W-Cu composites reinforced by copper coated graphene prepared using infiltration sintering and spark plasma sintering: A comparative study. *International Journal of Refractory Metals and Hard Materials*, 2019. 82: p. 91-99.
- [10] Shu-dong, L., et al., Microwave sintering W–Cu composites: Analyses of densification and microstructural homogenization. *Journal of Alloys and Compounds*, 2009. 473(1): p. L5-L9.
- [11] Tao, J. and X. Shi, Properties, phases and microstructure of microwave sintered W-20Cu composites from spray pyrolysiscontinuous reduction processed powders. *Journal of Wuhan University of Technology-Mater. Sci. Ed.*, 2012. 27(1): p. 38-44.
- [12] Yu, Y., W. Zhang, and H. Yu, Effect of Cu content and heat treatment on the properties and microstructure of W–Cu composites produced by hot extrusion with steel cup. *Advanced Powder Technology*, 2015. 26(4): p. 1047-1052.
- [13] Kim, S.-W., Y.-D. Kim, and M.-J. Suk, Micropatterns of W-Cu composites fabricated by metal powder injection molding. *Metals and Materials International*, 2007. 13(5): p. 391.
- [14] Luo, C., et al., The activated sintering of WCu composites through spark plasma sintering. *International Journal of Refractory Metals and Hard Materials*, 2019. 81: p. 27-35.
- [15] Pervikov, A.V., et al., Synthesis of W-Cu composite nanoparticles by the electrical explosion of two wires and their consolidation by spark plasma sintering. *Materials Research Express*, 2020. 6(12): p. 126519.
- [16] Guillon, O., et al., Field-Assisted Sintering Technology/Spark Plasma Sintering: Mechanisms, Materials, and Technology Developments. *Advanced Engineering Materials*, 2014. 16(7): p. 830-849.

Design of the Two-Wheeled Vehicle using Metal Hydride Vessels

Filip Duda¹, Natalia Jasminska², Ivan Mihalik³, Romana Dobakova⁴

Department of Power Engineering, Faculty of Mechanical Engineering, Technical University of Košice, Slovakia

*Corresponding Author

Received: 20 September 2022/ Revised: 05 October 2022/ Accepted: 12 October 2022/ Published: 31-10-2022

Copyright © 2021 International Journal of Engineering Research and Science

This is an Open-Access article distributed under the terms of the Creative Commons Attribution Non-Commercial License (<https://creativecommons.org/licenses/by-nc/4.0>) which permits unrestricted Non-commercial use, distribution, and reproduction in any medium, provided the original work is properly cited.

Abstract— Article describes the issue of hydrogen storage in the structure of metal alloys, solves design of metal hydride pressure vessel and solves the design of the concept of prototype two-wheeled vehicle powered by fuel cell with designed metalhydride pressure vessels.

Keywords— metal hydride, hydrogen, two-wheeler, fuel cell.

I. INTRODUCTION

Hydrogen is receiving more and more attention in Europe and around the world. The most important aspect is the fact that the energy recovery of green hydrogen in fuel cells produces no air emissions. Thus, it represents a possible solution to partially decarbonize industrial processes and economic sectors.

In the field of transport infrastructure, it is necessary to focus on alternative fuels and systems that will be created from renewable energy sources. Of course, these systems will also support the reduction of greenhouse gases. Currently, two technological platforms appear as long-term fuel sources, for example electromobility and hydrogen transport systems. Today, Slovakia has a commitment that more than 20% of vehicles in public administration should be free of combustion emissions in 2021.

Currently, hydrogen fuel is stored at extremely high pressures of 35-95 MPa. Today, there are options for storing hydrogen in various compounds that provide better storage options.

The implementation of hydrogen technologies with metal hydride reservoirs provides scope for increasing the safety and storage of H₂ at lower pressures. To be able to use this type of hydrogen storage, it is necessary to design a reservoir that will meet the working conditions.

II. DESIGN OF METALHYDRIDE PRESSURE VESSEL

When designing the pressure vessel, it is necessary to work with standard STN EN 13322-2. This standard provides a specification for gas transport vessels, the design and manufacture of refillable steel transport welded gas vessels, in this case the medium that will be used in the vessel is hydrogen.

This European standard describes the minimum requirements for the design, material, production processes and production tests of gas transport vessels welded from stainless steel with a water volume ranging from 0.5 to 150 litres for liquefied dissolved and compressed gases. The standard is only applicable to stainless steel vessels with a maximum tensile strength of up to 1100·106 Pa. The design of the reservoir consists of two main parts, and the primary reservoir, which contains the hydrogen-absorbing metal hydride alloy and the casings (Fig. 5). Between the primary reservoir and the case there is an intermediate space in which the coolant flows. Stainless steel type 1.4404 or 316L was chosen for the construction of the metal hydride reservoir with the mechanical properties listed in tab. 1. The use of the type of steel is prescribed by the standard.

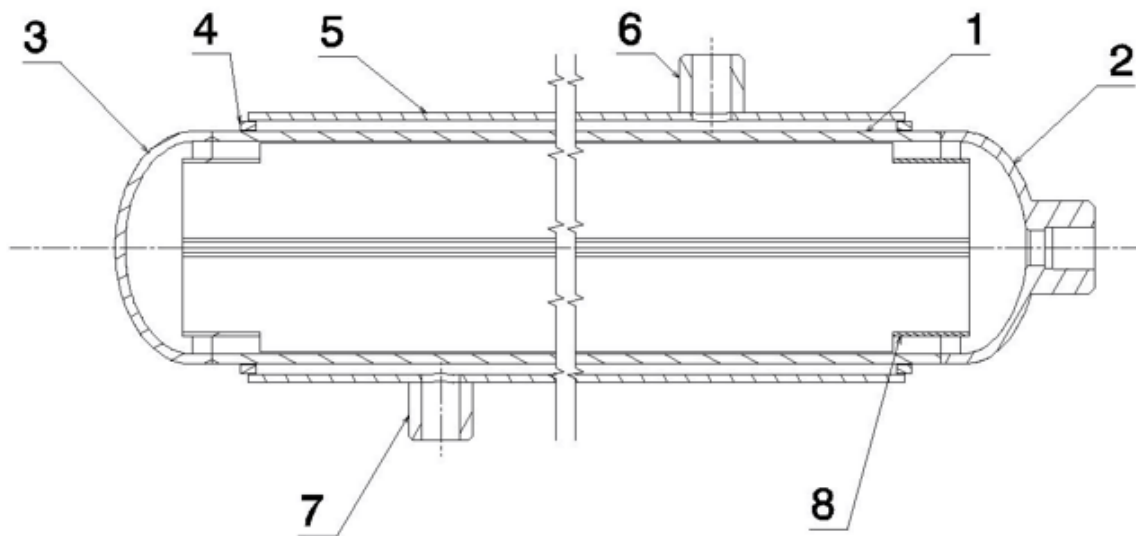
TABLE 1
MECHANICAL PROPERTIES OF STAINLESS STEEL 1.4404

0,2% Re(MPa)	Rm(MPa)	$\rho(\text{kg}\cdot\text{m}^3)$	μ	E(MPa)
200	500-700	8000	0,3	$2,1\cdot 10^5$

Where *Re*- Yield strength (MPa), *Rm*- tensile strength (MPa), ρ - density ($\text{kg}\cdot\text{m}^3$), μ - Poisson's number (-) and *E*- Young modulus of elasticity (MPa).

The process of hydrogen absorption into the structure of the metal hydride alloy is an exothermic reaction, during which heat energy is generated. Therefore, it is necessary to effectively cool the reservoir during its operation.

The reservoir can be cooled with active and passive modules. The active cooling module is the cooling liquid, in this case water, which is in the interspace between the primary pressure vessel and the case. The passive cooling module is located inside the primary pressure vessel and is a heat transfer intensifier that serves to increase the heat removal from the core of the tank in the direction of the fins to the wall of the primary vessel, where the vessel is cooled by water. By changing the geometry of the intensifier, it is possible to improve heat dissipation, thereby improving the absorption process. When designing the heat transfer intensifier, aluminium is considered because it has good thermal conductivity ($237 \text{ W}\cdot\text{m}^{-1}\cdot\text{K}^{-1}$).



1- cylindrical part of the primary vessel, 2- elliptical bottom with NPT1/4"thread, 3- elliptical bottom, 4- flange for casing, 5-cylindrical part of casing, 6- flange with G1/2 thread, which serves as the coolant supply, 7- flange G1/2, which serves as coolant drainage, 8- heat transfer intensifier

FIGURE 1: Design of metalhydride pressure vessel

III. APPLICATION OF A METAL HYDRIDE STORAGE VESSEL TO THE CONCEPT OF A TWO-WHEELED VEHICLE

The designed vessel with an internal heat transfer intensifier according to the STN EN 13322-2 standard was subsequently used in the design of the concept of a two-wheeled mobile device, using metal hydride alloys and a fuel cell for propulsion. The proposed device is shown in Fig. 2. The device is a hybrid that is powered by electricity and a fuel cell. A fuel cell is an electrochemical device that converts the chemical energy of the fuel and oxidizer directly into electrical energy. A Horizon 500 PEM proton exchange membrane (PEM) fuel cell was used for the design of the mobile device. The parameters of the selected fuel cell in the two-wheeler concept are listed in table 2.



FIGURE 2: Concept of a hybrid two-wheeler powered by a fuel cell and an electric motor

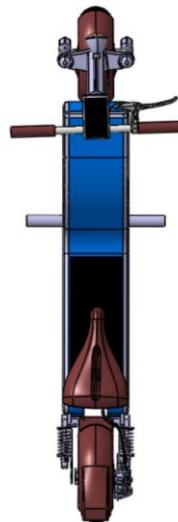


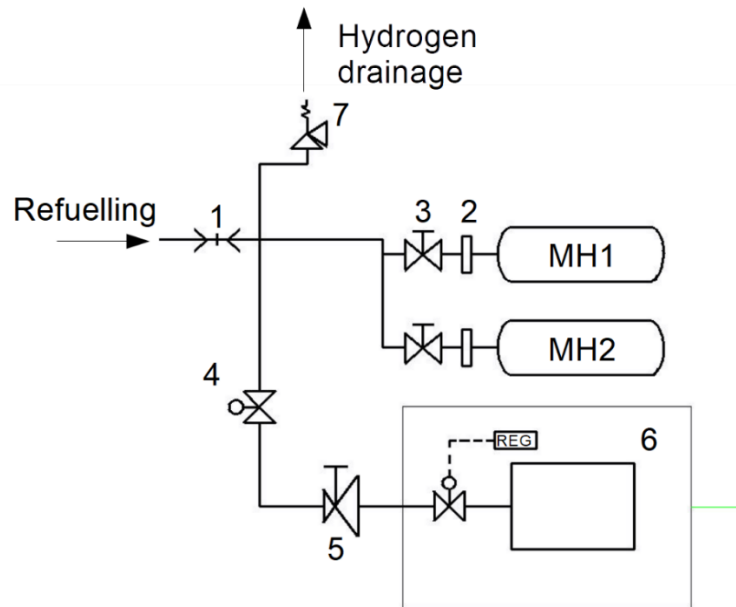
FIGURE 3: Top view of the designed device

TABLE 2
PARAMETERS OF SELECTED FUEL CELL

Number of cells	24
Nominal power	500 W
Power	14.4V 35A
Hydrogen supply valve voltage	12 V
Flush valve voltage	12 V
Fan voltage	12 V
Reactants	Hydrogen and air
Ambient temperature	5 - 30°C
Maximum device temperature	65 °C
Total weight of the device	2,5 kg

The base of the designed device is formed by a duralumin frame. In the device, a 500 W motor located in the rear wheel, a battery with a capacity of 48 V and 14.4 Ah and a control unit are considered. The concept envisages front and rear wheel suspension to minimize vibration of the base plate, which houses the fuel cell. The brake system is located on the rear wheel of the device. After adding up all the parameters, the total weight of the device is approximately 28 kg.

The metalhydride vessels used in the design of the device have length 300 mm and the diameter of vessel is 60 mm. In Tab. 3 shows the individual parameters of the vessels used in the draft concept. In Fig. 4 it is possible to see the designed hydrogen circuit in the device.



MH1 and MH2 represent the used MH vessels within the design, 1- refuelling neck, 2- filter, 3- manual valve, 4 - Solenoid valve, 5- reducing valve, 6- fuel cell and regulation, 7- hydrogen drainage.

FIGURE 4: Hydrogen circuit in designed two-wheeler

**TABLE 3
PARAMETERS OF USED METALHYDRIDE PRESSURE VESSELS**

Volume of metalhydride	1,232 · 10 ⁻³ m ³
Weight of metalhydride	3,6 kg
Weight of stored hydrogen	0,05 kg
Volume of hydrogen	0,597 m ³
Generated heat	6154,43 kJ

Based on the values from Tab. 3, it is possible to calculate the maximum range of the designed device.

The maximum range of the designed device is obtained from equation:

$$m_{H_2} \cdot Q_m = X \tag{1}$$

(kJ)

where: Q_m is calorific value of hydrogen ($Q_m = 119\,550$ kJ), m_{H_2} is the mass of stored hydrogen in the metalhydride alloy, X is total heat generated in pressure vessels.

After substituting the mass of hydrogen and calorific value of hydrogen into equation (57), the total heat generated in the reservoirs is 6154,43 kJ. The efficiency of the used fuel cell is 0.5, which means that the total heat released from the fuel cell is 3077.22 kJ. The nominal power of the fuel cell is $0,5 \text{ kJ}\cdot\text{s}^{-1}$.

$$t_p = \frac{Q}{P} \quad (\text{s}) \quad (2)$$

where t_p - maximum time of operation of the fuel cell, Q - released heat from the fuel cell, P - nominal power of the fuel cell.

After dividing the heat released by the fuel cell and the nominal power (2), the obtained time is 102 min. This time represents the maximum operating time of the fuel cell.

The next step is the calculation of the maximum operating time of the device on the battery and electric motor. The battery capacity was determined from the equation:

$$c = Q \cdot U \quad (\text{Wh}) \quad (3)$$

where: c is capacity (Wh), Q is electric charge (Ah), and U is a voltage (V). Battery in device has 14,4 Ah and 48 V.

After substituting the voltage and electric charge into equation (3), the battery capacity is 691.2 Wh. The maximum operating time of the electric engine was calculated from the equation (4):

$$t_e = \frac{c_{\text{battery}}}{P_{\text{el.engine}}} \quad (\text{s}) \quad (4)$$

Where: t_e - maximum operating time of the electric engine and battery (s), c_{battery} - capacity of the battery (Wh), $P_{\text{el.engine}}$ - power of electrical engine (W)

After substituting the battery capacity and the power of the electric motor into equation (4), the maximum operating time of the electric motor and battery is 80 min.

The maximum range of the device is obtained from the equation:

$$s = v \cdot t_c \quad (\text{km}) \quad (5)$$

Where s - distance (km), v - average speed of device ($\text{km}\cdot\text{h}^{-1}$) a t_c -total operation time (h).

The total operating time of the device is obtained as the sum of the maximum operating times of the fuel cell and the electric engine with the battery.

$$t_c = t_p + t_e \quad (\text{s}) \quad (6)$$

Where t_c - the total operating time of the device.

The total operating time of the designed device is 3.03 h. The average speed of the device is $25 \text{ km}\cdot\text{h}^{-1}$. After substituting the average speed and total operating time into equation (5), the maximum range of the device is obtained, which is approximately 75 km under optimal conditions. This means when there is no wind, at zero slope and at room temperatures.

IV. CONCLUSION

The main task of this work was to design a two-wheeled device that uses a type of hydrogen storage based on absorption into the metal alloy structure. It is also a hybrid two-wheeled device using a fuel cell and an electric motor, whose estimated range based on calculations is approximately 75 km. The next step of this work will be the construction of a real functional prototype and subsequent testing of the designed metal hydride vessels in this device.

ACKNOWLEDGEMENTS

This paper was written with the financial support from the VEGA granting agency within the project solutions No. 1/0626/20 and No. 1/0532/22 from the KEGA granting agency within the project solutions No. 012TUKE-4/2022 and with financial support from the granting agency APVV within the Project Solution No. APVV-15-0202, APVV-21-0274 and APVV-20-0205.

REFERENCES

- [1] Jose Bellosta von Colbe; Application of hydrides in hydrogen storage and compression: Achievements, outlook and perspectives, International Journal of Hydrogen Energy, strany 7780-7808, 2019.
- [2] Mykhaylo Lototsky; Metal hydride hydrogen storage tank for fuel cell utility vehicles, International Journal of Hydrogen Energy, strany 7958-7967, 2020.
- [3] STN EN 13322-2, Prepravné fľaše na plyny. Navrhovanie a výroba znovuplniteľných ocelových fliaš na plyny. Časť 2: Nehrzdavejúce ocele, 2003
- [4] Jurczyk, Mieczyslaw.: Handbook of Nanomaterials for Hydrogen Storage. Singapore: Pan Stanford Publishing Pte. Ltd, 2018. ISBN 978-1-315-36444-5.
- [5] Sankir, M a Sankir, D, N.: Hydrogen Storage Technologies. Scrivener Publishing LLC, 2018. ISBN 978-1-119-45988-0.
- [6] Stolten, D.: Hydrogen and Fuel Cells, Weinheim: Wiley, 2010, 908 s. ISBN 978-3-527-32711-9.
- [7] Tóth, L., T. Brestovič a N. Jasminská.: Absorption of Hydrogen in the HBond©9000 Metal Hydride Tank, International Journal for Innovation Education and Research, 2018.

Suitability of using Silica Gel in Powder Form as an Adsorbent in the Drying Process

Romana Dobakova¹, Filip Duda^{2*}, Ivan Mihalik³, Tomas Brestovic⁴

¹Department of Power Engineering, Faculty of Mechanical Engineering, Technical University of Kosice, Slovakia

*Corresponding Author

Received: 24 September 2022/ Revised: 06 October 2022/ Accepted: 14 October 2022/ Published: 31-10-2022

Copyright © 2021 International Journal of Engineering Research and Science

This is an Open-Access article distributed under the terms of the Creative Commons Attribution Non-Commercial License (<https://creativecommons.org/licenses/by-nc/4.0>) which permits unrestricted Non-commercial use, distribution, and reproduction in any medium, provided the original work is properly cited.

Abstract— Gases used in industry must meet the required parameters such as the content of gas impurities, moisture content and mechanical impurities, which have a significant impact on its subsequent use. Various industrial drying methods are used to remove moisture. Among the most used drying methods are methods based on subcooling the gas below the condensation temperature, adsorption drying methods or special methods. The article primarily deals with the drying of gases in a fluid layer of ground silica gel. It describes the issue of the suitability of silica gel as an adsorbent in any form of its structure, the advantages and disadvantages of its use.

Keywords— silica gel, adsorption, drying.

I. INTRODUCTION

The drying process is a complicated physical process, in which the effect of heat reduces the liquid content in the substance, without changing its chemical composition.

The essence of drying is the migration of moisture in the opposite direction to the sorption process. During the general drying process, moisture moves from the porous core of the material to the surface layers and into the surrounding environment, whereupon the moisture meets the drying medium, which carries it away.

To determine the most optimal drying conditions, it is necessary to know the physical laws that affect drying in the individual phases of the entire process, the input parameters and the required performances.

II. SILICA GEL AS ADSORBENT

The principle of adsorption is the ability of some porous solid substances to bind gas particles or liquid substances on their surface. Trapped substances are released by desorption and the adsorbent can return to the process. The adsorbed amount depends not only on the nature of the adsorbing gas, but also on the nature of the solid substance, on the size of the surface, on the partial pressure of the adsorbing component in the gas phase, and on the temperature. During adsorption, it is important that the adsorbent has as large an active surface as possible.

Known adsorbents include silica gel. It is a granular, porous form of silica, produced synthetically from sodium silicate and sulfuric acid in the form of hard irregular grains or regular balls. The porous structure of interconnected cavities provides a very high surface area (up to $800 \text{ m}^2 \cdot \text{g}^{-1}$), which allows water vapor to be easily adsorbed. Thanks to this feature, it can be used for example when drying gases. Ordinary silica gel binds an amount of water corresponding to approximately 20% of its weight. Even when saturated with water vapor, silica gel still has the appearance of a dry product, and its shape remains unchanged. After being saturated with water, it can be regenerated again by heating to the appropriate temperature (approx. $150 \text{ }^\circ\text{C}$). Aluminium oxide is added to increase its water resistance.

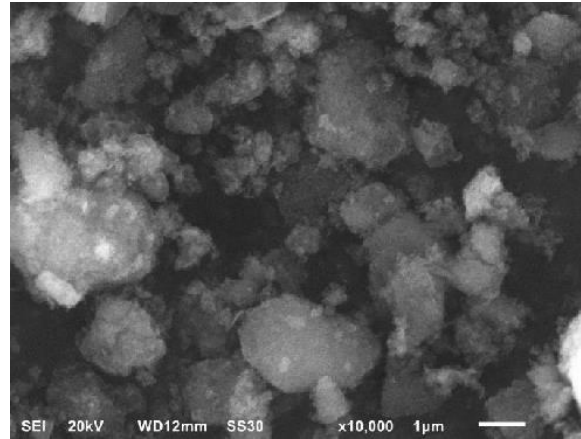


FIGURE 1: Structure of silica gel [6]

Silica gel is non-toxic, non-flammable and chemically highly inert. Sometimes it comes with a moisture indicator admixture that will change its colour whenever it is wet.



a) Type N – normal grains



b) Type WS – water resistant grains



c) Type Orange gel – indicator grains

FIGURE 2: Types of silica gel

III. DESCRIPTION OF THE MEASUREMENT PROCESS AND DESIGN OF THE EXPERIMENTAL EQUIPMENT

For the purposes of the experiment, spherical silica gel was ground into a fine powder with the help of a crushing mill, while the grain size of the particles was in the range of 0.004 - 0.08 mm (Fig. 3). The structure of the sample was observed using a BRESSER microscope (Fig. 4). Hydrogen was used as the gas that caused the levitation of silica gel particles and the subsequent formation of a fluid layer. This gas was simultaneously subjected to experimental drying.



FIGURE 3: Ground sample of silica gel

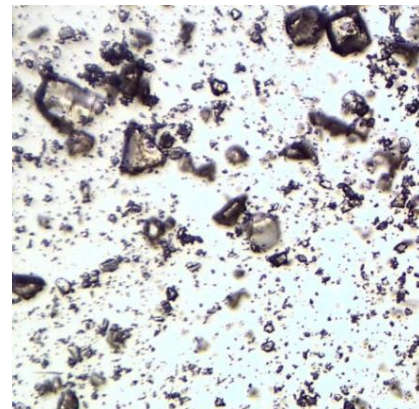
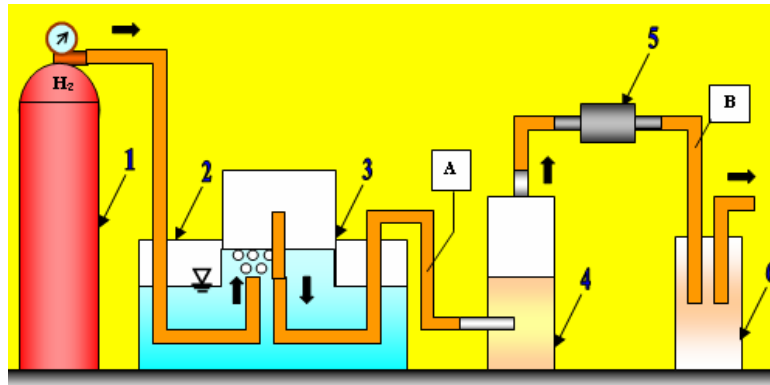


FIGURE 4: The structure of silica gel under a microscope

The model of the designed device for determining the efficiency of silica gel drying is shown in fig. 5. When measuring the required quantities, it was based on two measurement points - point A and B.



1 – pressure vessel, 2 – outer container, 3 – measuring cylinder, 4 – container with silica gel, 5 – filter, 6 – drain container SiO₂

FIGURE 5: Model of experimental equipment

The used hydrogen subjected to drying was stored in a pressure vessel 3.0. The pressure vessel has a gas purity of 99.999% and residual impurities are 0.001% (water vapor, oxygen, nitrogen, CO, CO₂, hydrocarbons).

Dry hydrogen gas was discharged from the pressure vessel into a vessel with water, where it was subsequently moistened using a levelling device (outer vessel and measuring cylinder). By bubbling hydrogen through the water, it was moistened. Subsequently, the humidified gas proceeded through the part where the sensor recording the gas humidity was placed, into a container with silica gel placed in a cylinder-shaped vessel with a total height of 0.02 m, made of PVC. The diameter of the vessel was 0.046 m.

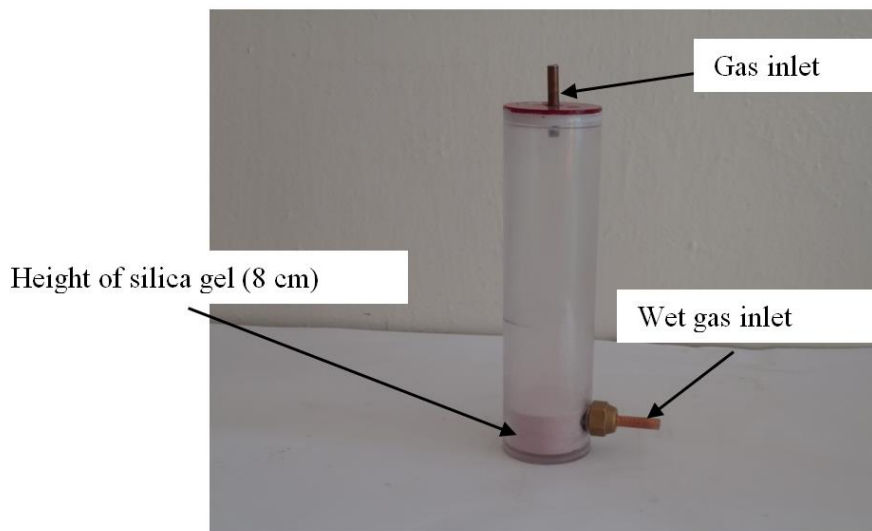


FIGURE 6: Vessel with silica gel

After entering the container, the hydrogen formed a fluid layer of silica gel, and at the same time it dried. After passing through the container with silica gel, the hydrogen passed through the filter, which had the task of capturing silica gel particles that were carried by the gas stream, to the part where the sensor recording the humidity of the gas was placed.

IV. EVALUATION OF EXPERIMENTAL MEASUREMENT RESULTS

During the measurement, the values of the relative humidity of hydrogen and the temperature during its flow through the constructed experimental device were recorded. To determine these quantities, we used a measuring device from the manufacturer Ahlborn - ALMEMO 2390-5 and a relative humidity and air temperature sensor FHA646. The results were subsequently processed using the AMR-Control software on a PC.

The measurement at point A was made in front of a cylinder filled with silica gel. The time interval was 10 seconds, and the measured values are shown in fig. 7.

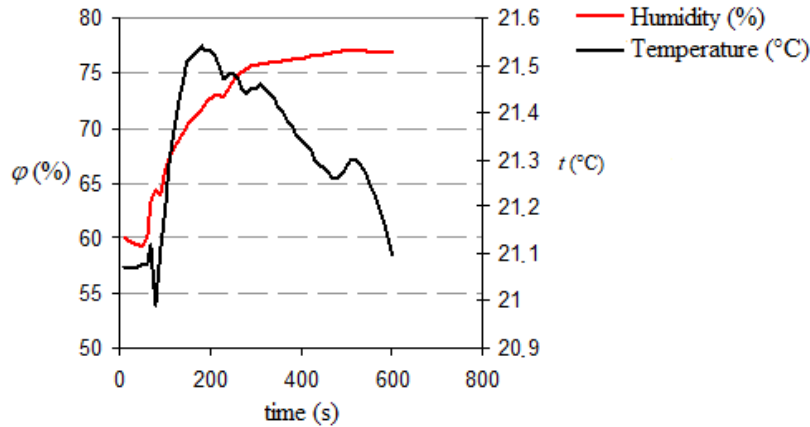


FIGURE 7: Dependence of relative humidity and temperature at measuring point A

The highest temperature value during the measurement was 21.54 °C and humidity 77%.

The measurement at point B was made behind the filter. The time interval was 10 seconds, and the measured values are shown in fig. 8.

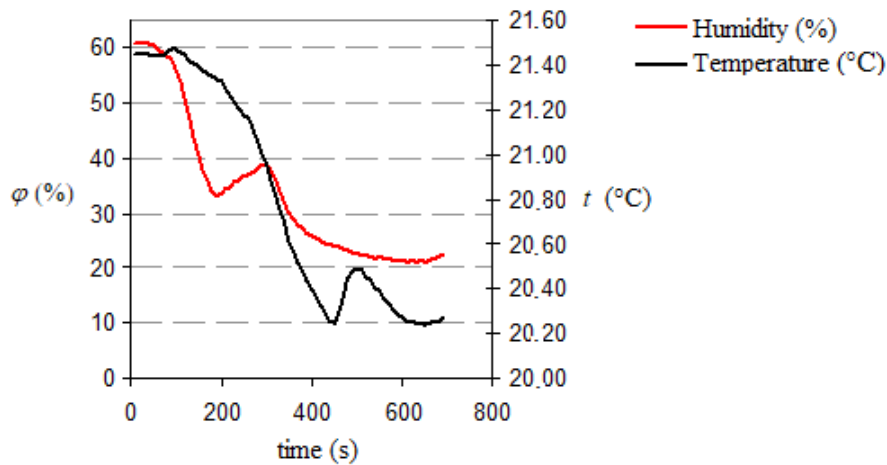


FIGURE 8: Dependence of relative humidity and temperature at measuring point B

The minimum temperature value was 20.4 °C and humidity 21.1% and the maximum measured temperature was 21.47 °C and humidity 60.8%.

To check and verify the appropriateness of using the gas drying method in a fluid layer of silica gel, the measurement was also carried out with classic non-ground silica gel (ball shape). The measurement was carried out on a constructed experimental device without the inclusion of a filter.

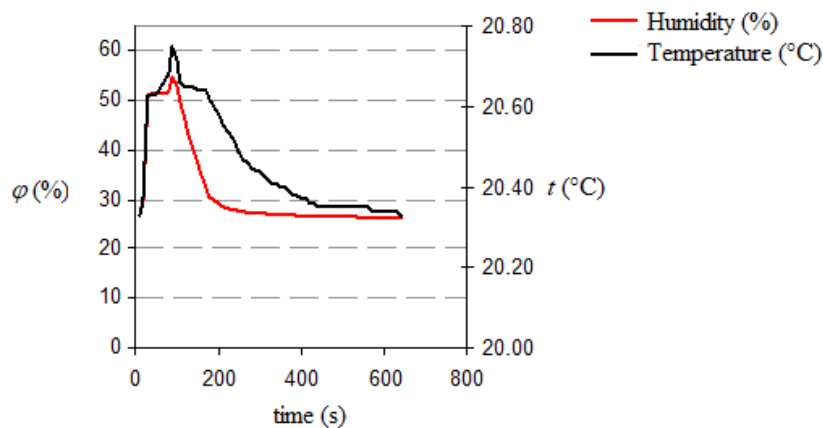


FIGURE 9: Dependence of relative humidity and temperature of unground silica gel at measuring point B

According to the measured values, a relative humidity value of 21.1% was achieved in connection with a filter device, with the method using unground silica gel the value was 26.3%, meaning 5.2% lower.

V. CONCLUSION

The use of ground silica gel as an adsorbent has both advantages and disadvantages compared to classic silica gel. From an economic point of view, the drying method with the classic structure of silica gel is more advantageous, since the initial costs of changing its structure (grinding in a crushing mill) are eliminated, as well as the need to use a high-efficiency filter device. Another disadvantage of using ground silica gel is its lower weight, which makes it easier to drift. There is an increase in the height of the fluid layer, which reduces the density of the particles and the gas flows more easily around the dispersed particles. As a result of this phenomenon, their direct contact does not occur, which can be explained by the relatively high range of minimum and maximum measured humidity.

Since it was found by measurement that the removal of moisture from the gas using the method with ground silica gel and the classic structure represents a difference of only 5.2%, the drying method with classic silica gel is preferable, taking into account both economic and health aspects in the operation process. Ground silica gel carried by the air stream also has a significant impact on the life of filters, which tends to clog and reduce gas flow. Particles that are not caught by the filter can clog other parts of the device, as well as measuring instruments, which can subsequently be damaged and the given output parameters of the measured quantities can be distorted.

ACKNOWLEDGEMENTS

This paper was written with the financial support from the VEGA granting agency within the project solutions No. 1/0626/20 and No. 1/0532/22 from the KEGA granting agency within the project solutions No. 012TUKE-4/2022 and with financial support from the granting agency APVV within the Project Solution No. APVV-15-0202, APVV-21-0274 and APVV-20-0205.

REFERENCES

- [1] Yan, K. L. and Wang, Q.: Adsorption characteristics of the silica gels as adsorbent for gasoline vapors removal. IOP Conf. Series: Earth and Environmental Science, 153 (2018), 022010.
- [2] Grande, C. A. et. al.: Silica Gel as a Selective Adsorbent for Biogas Drying and Upgrading. Ind. Eng. Chem. Res, 59 (2020), p. 10142–10149.
- [3] Mourik, J.: Experiences with Silica Gel as Adsorbent. American Industrial Hygiene Association Journal, 26 (5) (2007), p. 498 – 509.
- [4] Scherer, G. W.: Effect of drying on properties of silica gel. Journal of Non-Crystalline Solids, 215 (2-3) (1997), p. 155 -168.
- [5] Mujumdar, A.S.: Principles, Classification, and Selection of Dryers. Handbook of Industrial Drying. CRC, (2006). p. p. 1279.
- [6] Song, Z., Zhao, H.: Preparation and Characterization of Mullite-Silica Aerogel Composite Material. Open Journal of Organic Polymer Materials, 8 (4) 2018, p. 43 – 52.

Yeast Strains from *Burukutu* and *Fura*, as an Alternative for Commercial Baker's Yeast

Umeh, S.O.^{1*}; Igwilo, I.O.²; Okafor, U.C.³; Agbara, A.C.⁴; Ezech F. N.⁵

^{1,3}Department of Applied Microbiology and Brewing, Nnamdi Azikiwe University, Nigeria

²Department of Applied Biochemistry, Nnamdi Azikiwe University, Nigeria

⁴Department of Biochemistry, Ebonyi State University, Abakaliki, Nigeria

⁵University of North Texas, Denton, TX 76203, USA.

*Corresponding Author

Received: 30 September 2022/ Revised: 09 October 2022/ Accepted: 18 October 2022/ Published: 31-10-2022

Copyright © 2021 International Journal of Engineering Research and Science

This is an Open-Access article distributed under the terms of the Creative Commons Attribution

Non-Commercial License (<https://creativecommons.org/licenses/by-nc/4.0>) which permits unrestricted

Non-commercial use, distribution, and reproduction in any medium, provided the original work is properly cited.

Abstract— Baker's yeast has been employed in the manufacturing of bread for at least 6,000 years ago. They are responsible for dough leavening and without them sugar in the dough will not be reduced and the substrate will be left unleavened. They have been identified by Scientists as *Saccharomyces cerevisiae* and are easily obtainable from fermenting fruits and beverages of high carbohydrate content. This work was carried out to determine the possibility of isolating baker's yeast from two local drinks, *Burukutu* and *Fura*. The drinks were prepared and allowed to ferment for 72hrs and cultured on Sabouraud Dextrose Agar (SDA) plates incorporated with chloramphenicol for 48hrs. Colonies that grow were counted and sub-cultured on Yeast Peptone Dextrose (YPD) Medium for 72hrs. Discrete colonies were sub-cultured, stored, identified and characterized. Their attributes as baker's yeast such as ethanol and stress tolerance, flocculation, hydrogen sulphide production, temperature tolerance and fermentative ability were determined. Results showed that two isolates were selected and identified as 'Isolated yeast from *burukutu* (IYB), Isolated yeast from *fura* (IYF)'. They showed similar microscopic appearance with reconstituted conventional commercial baker's yeast (CCY) such as the presence of ellipsoidal to oval cells with multipolar buds and ascospores. The multipolar buds were highest in IYB and lowest in CCY. Yeast count ranges from 3.7×10^3 to 2.8×10^3 colony forming unit per millilitre (cfu/ml). All the isolates were able to tolerate different concentrations of ethanol and temperature regimes at varying intensities. None of the isolates produced hydrogen sulphide but show intense to moderate response to stress, flocculation and fermentative ability. Local beverages (*Burukutu* and *Fura*) are therefore recommended to be good sources of baker's yeast which can compare favourably with the conventional commercial baker's yeast.

Keywords— *Burukutu*, *Fura*, *Saccharomyces cerevisiae*, Baker's yeast.

I. INTRODUCTION

Baker's yeast had been and is still an inevitable component of raw materials used by bakers all over the world. They ferment, leaven or increase the volume of dough mixed for bread and other confectionary products through gas (CO₂) incorporation. They do not only increase the volume of the dough through carbohydrate utilization and gas incorporation but also help in creating the desired flavour and texture in the dough (Fleury *et al.*, 2002; Umeh *et al.*, 2019; Sergei, 2020; Casas-Godoy *et al.*, 2021). During fermentation process in the dough, large quantity of CO₂ is produced. Baker's yeast had been identified by researchers as *Saccharomyces cerevisiae* and is the most commonly used species of *Saccharomyces* in bread baking. It has been employed as baker's yeast in manufacturing bread for at least 6,000 years ago (Kevin, 2005; Sergei, 2020; Casas-Godoy *et al.*, 2021).

In Nigeria and some countries, Baker's yeast is only obtained by importation from Europe or America due to the delicate means of preservation. They are mainly used as dried, preserved as powders and are delicate to handle. Researchers had deduced that *Saccharomyces cerevisiae* does not inhabit any other environment except nature. They can be isolated from vinery environment as wild or domesticated species (Martin *et al.*, 1993; Mortimer, 2000; Umeh *et al.*, 2019). Kurtzman and Fell (1998) reported that fruits, vegetables, drinks and agricultural products are among the important micro habitats for wild yeasts.

Yeast strains are known to inhabit foods and beverages (Graham, 2007). They play an important role in the fermentation process. *Saccharomyces cerevisiae* is employed in the production of wine, beer, bread and alcoholic beverages (Mortimer, 2000; Sergei, 2020; Grijalva-Vallejos *et al.*, 2020). Alcoholic drinks had been found to be good sources of *Saccharomyces cerevisiae* (Kurtzman and Fell, 1998; Graham, 2007; Umeh *et al.*, 2015; Agwuna *et al.*, 2019)

Alcoholic beverages consumed in some states in Nigeria were produced locally and can be sources of domesticated yeasts like *Saccharomyces cerevisiae*. Such beverages include *Burukutu* (local sorghum beer) and *Fura* (Millet meal). These drinks are always available at all seasons of the year. Their raw materials and methods of preparation are cheap and easily available.

Baking industry is very costly in Nigeria, due to the high cost of imported bakers' yeast from developed countries, a process that drains its foreign reserve (Yabaya and Jatau, 2009, Umeh *et al.*, 2019). The scarcity of bakers' yeast has resulted in poor production of bread by bakers and making consumption of good quality bread almost beyond reach to low income earners (Yabaya and Jatau, 2009). Sometimes the imported yeasts when reconstituted fail to possess the attributes of the required species thereby rendering the production invaluable.

There is great need to look into the potentials of local beverages as sources of the yeasts that can possess the characteristics of baker's yeast to be used in our baking and confectionary industries.

II. MATERIALS AND METHODS

2.1 Sample collection

"*Burukutu*" (local sorghum beer) was obtained from a local seller at Aroma Junction, Awka with a sterile plastic container and immediately transported to the laboratory of the Department of Applied Microbiology and Brewing, Nnamdi Azikiwe University, Awka.

Millet meal (*Fura*) and Commercial bakers' yeast were purchased from Eke Awka market in a sterile plastic container and cellophane bag respectively and also transported to the laboratory.

Culture media, chemicals and reagents were purchased from Head Bridge Drug Market in Onitsha, Anambra State. All the chemicals and reagents are of analytical grade and unadulterated.

2.2 Yeast Isolation and Identification

The method of Chiranjeev *et al.*, (2013) as modified and used by Umeh *et al.*, (2019) was adopted for the isolation and identification of yeasts from the *burukutu* and *fura* samples. This was done by pour plating of serially diluted samples of the *burukutu* and *fura* differently on separate plates of Sabouraud dextrose agar (SDA) incorporated with chloramphenicol. The plates were incubated at room temperature ($27\pm 2^{\circ}\text{C}$) for 48hrs and the developed colonies counted. The different developed colonies were sub-cultured on fresh Potato Dextrose agar (PDA) plates, incubated at same condition for 72hrs to get pure cultures of the yeast strains. The isolated yeast strains were characterized and preliminarily identified using colony morphology, cellular characteristics, ascospore formation, vegetative reproduction and sugar utilization. The isolates were identified further preliminarily using the Fungal Atlas by comparing them with known taxa. They were then stored in a slant and preserved in the refrigerator at 4°C for further genomics and gene sequencing identification using and usage.

2.3 Examination of the Isolates for Attributes of Baker's Yeast

The methods of Chi and Ameborg, (2000) as used by Umeh *et al.*, (2019) were used to check the isolates for their attributes as baker's yeast. The following attributes were determined:

2.3.1 Ethanol Tolerance test

The ability of the isolated strains to grow and survive in high concentrations of ethanol was tested by growing them in Yeast Peptone Glucose (YPG) broth containing three different concentrations of ethanol. One loop full of each isolate was inoculated into freshly prepared YPG broth, containing ethanol concentrations of 10, 15 and 20% (v/v) respectively and incubated for 72hrs and observed for survival and multiplication.

2.3.2 Stress Tolerance

The ability of the isolates to survive at different stress conditions was done for consecutive 15 days' inoculation and incubation on different media. This was conducted by first growing the isolates on normal YPG for 3days, then transferring them on YPG

medium containing 8% (v/v) ethanol and 20% (w/v) glucose for another 3 days and finally inoculating them on YPG medium with 8% (v/v) ethanol and 20% ((w/v) sucrose for the last 3 days, all incubated at the same condition of temperature.

2.3.3 Flocculation Test

A loop full of each of the isolates was inoculated in a test tube containing 10 ml fresh YPG broth and incubated at 30°C for 72hrs. The tubes were observed after 72hrs and agitated to observe flocculate formation.

2.3.4 Hydrogen sulphide production

The ability of the isolated yeasts to produce hydrogen sulphide was checked by growing them on Lead acetate medium which is composed of 40 g/l Glucose, 5 g/l Yeast extract, 3 g/l Peptone, 0.2 g/l Ammonium sulphate, 1 g/l Lead acetate and 20 g/l Agar. The set up was incubated for 30 °C for 10 days and the media tested for the presence of hydrogen sulphide.

2.3.5 Temperature Tolerance Test

The ability of the isolates to grow at varying degrees of temperatures was checked by culturing them on YPG medium and incubating them at three different temperature regimes of 30 °C, 35 °C and 45 °C. The isolates were streaked on the medium and incubated for 72hrs.

2.3.6 Fermentative ability

The ability of the isolates to ferment different carbon sources was checked in this test. Solutions of 10 ml 6 % (w/v) each of glucose, sucrose, fructose, galactose, raffinose, lactose and maltose were autoclaved differently with inverted Durham tubes and cooled. The isolates were each grown on YPG at 30 °C for 72hrs. They were then inoculated on fresh Yeast fermentation broth (YFB) made of 7.5 g/l Peptone, 4.5 g/l Yeast extract, and 1 ml of 1.6% (w/v) Bromothymol blue as indicator. Equal quantities of the YFB were aseptically added to each of the tubes containing the different carbon sources and 2 loop fill of each isolate inoculated. They were incubated at 30 °C for 72hrs and the tubes examined for turbidity, acid and gas formation.

III. RESULTS

The isolates were identified and designated as Isolated yeast from *burukutu* (IYB), and Isolated yeast from *fura* (IYF) while the Conventional commercial yeast was designated as CCY. They show the same type of microscopic appearance of presence of ellipsoidal to oval cells with multipolar buds and ascospores. The multipolar buds were highest in IYB and lowest in CCY. Yeast count ranges from 3.7X10³ to 2.9X10³ colony forming unit per millilitre (cfu/ml) as shown in Table1.

**TABLE 1
COLONY MORPHOLOGY OF THE ISOLATES ON YPD AND YEAST COUNTS ON SDA**

Isolates	Creamy	fluffy	Smooth	Rough	Yeast counts X10 ³ cfu/ml
IYB	-	+	-	+	3.7
IYF	-	+	+	+	2.9
CCY	-	+	-	+	2.8

Key: - (Negative reaction), + (Positive reaction), cfu/ml (Colony forming unit per millilitre)

The isolates were able to tolerate different concentrations of ethanol and survive different temperatures regimes at varying intensities as presented in Table 2.

**TABLE 2
ETHANOL AND TEMPERATURE TOLERANCE ABILITY OF THE ISOLATED STRAINS**

Isolates	Ethanol concentrations (%)			Varying temperatures (°C)		
	10	15	20	30	35	40
IYB	+++	+++	+++	+++	++	++
IYF	+++	+++	++	+++	++	+
CCY	+++	++	++	+++	+	+

Key: +++ (Intensive growth) ++ (Moderate growth) + (Low growth)

Table 3 showed the results of stress exclusion test, flocculation, hydrogen sulphide production and fermentative abilities of the isolates.

TABLE 3
STRESS TOLERANCE, FLOCCULATION ABILITY, HYDROGEN SULPHIDE PRODUCTION AND FERMENTATIVE ABILITY OF THE ISOLATES.

Isolates	Stress Tolerance	Flocculation	H ₂ S production	Fermentative ability
IYB	+++	+++	-	+++
IYF	+++	++	-	+++
CCY	+++	++	-	++

Key: +++ (*Intensive response*) ++ (*Moderate response*) + (*Low response*)

The isolated yeasts and the conventional baker's yeast were able to ferment glucose, sucrose, fructose, galactose, and maltose with extensive to moderate gas production. None of the yeasts were able to ferment raffinose and lactose (Table 4).

TABLE 4
SUGAR FERMENTATION ABILITIES OF THE THREE ISOLATES

Isolates	Glucose	Sucrose	Fructose	Raffinose	Galactose	Lactose	Maltose
IYB	+	+	+	-	+	-	+
IYF	+	+	+	-	+	-	+
CCY	+	+	+	-	+	-	+

Key: + (*Able to ferment*) - (*Unable to ferment*)

IV. DISCUSSION

Baker's yeast had been identified by researchers as *Saccharomyces cerevisiae* (Benitez *et al.*, 1996; Thais *et al.*, 2006; Umeh *et al.*, 2019). The primary role of this yeast in baking is in dough development where it ferments the carbon source in the dough with simultaneous production of carbon dioxide thereby raising/leavening the dough. Without baker's yeast the fermentation and leavening of the dough would be impossible. Importation of baker's yeast had rendered some baking and confectionary industries weak in production due to its high cost. Most times, due to long storage, mutation of the yeasts may occur in transit rendering the yeast unsuitable for use and great loss to the producer. It had also led to high cost of bread and other backed products as the cost as well as the cost of baking flour are increasing day after day (Umeh *et al.*, 2017; Agwuna *et al.*, 2019).

Two Nigerian fermenting local beverages (*burukutu* and *fura*) were assessed for the presence of the baker's yeast. The two fermenting drinks when cultured on Sabouraud Dextrose Agar, showed the presence of fungal colonies after 48hrs. From the discrete colonies, the yeasts were isolated and selected based on their morphology, microscopic appearances and biochemical characteristics and enriched as baker's yeast (Table 1). Their colony appearances of Creamy, Fluffy, Smooth and rough/regular were attributes of known baker's yeast. This was in agreement with the report of Cavalieri *et al.*, (2001), Kuthan *et al.*, (2003), Kevin (2005) and Umeh *et al.*, (2019). The isolated yeast cells showed profuse budding capacity which is also a good feature of industrial baker's yeasts (Umeh and Okafor 2017). Colony growth on Sabouraud dextrose agar and yeast Peptone Agar were profuse and colony count much more than the reconstituted commercial yeast (Table 1). The conventional commercial yeast may show the same count range if higher dilution was cultured.

Table 2 showed the result of ethanol and temperature tolerance of the yeasts. All the three yeasts were able to withstand ethanol concentrations of 10% and grow profusely, the two isolated in the research grew profusely at 15% ethanol while the commercial baker's yeast showed moderate growth at 15% ethanol concentration. This is in line with the findings of Iraj *et al.*, (2002), Irena *et al.*, (2005) and Chilaka *et al.*, (2010). They also grow well at temperatures of 30 °C showing profuse growth, IYB and IYF grew moderately at 35 °C and scanty at 45 °C while CCY grew scanty at these temperatures (Table 2). This report supported the findings of Chiranjeev *et al.*, (2013) which said that yeast isolated from local/natural sources can survive high temperature regimes.

Both the yeasts isolated from the research and the commercial baker's yeast did not produce hydrogen sulphide on growth on yeast peptone glucose medium (Table 3). This is a good attribute of good baker's yeast as postulated by Irena *et al.*, (2005), Chilaka *et al.*, (2010) and Umeh and Okafor, (2016). The studied yeast strains were able to withstand stress on culturing them on media of different harsh conditions. IYB and IYF showed intensive growth under stress for 15 days while CCY show moderate growth response. IYB developed better flocculation in broth than IYF and CCY which developed scanty flocculates (Table 3). Baker's yeast tolerance to stress and ability to flocculate had been found to be good characteristics of baker's yeast as found and confirmed by Irena *et al.*, (2005) and Chilaka *et al.*, (2010). These two characteristics of baker's yeast help them to survive in different ingredients in the dough mixture without denaturing and at the same time do the function dough leavening (Umeh and Okafor, 2016).

The isolated yeasts in this research, Isolated *burukutu* and Isolated *fura* yeasts (IBY and IFY respectively) were able to ferment the tested carbohydrate sources (glucose, fructose, sucrose, galactose and maltose) but did not ferment raffinose and lactose. This is in line with the findings of Thais *et al.*, (2006) and Umeh *et al.*, (2019). Tarek (2001) reported that the *Saccharomyces cerevisiae* strains that do not ferment lactose lack the enzyme lactase or β -galactosidase system. The studied yeast species from this fermented the carbon sources with the production of gas. The gas produced was carbon dioxide which represents the carbon dioxide released during fermentation and leavening processes in bread making and this is paramount in bakery (Thias *et al.*, 2006).

V. CONCLUSION

The two local drinks studied showed good sources of baker's yeasts which competes and is found to be more potent than the conventional baker's yeast. These isolated yeasts can be potentially employed in baking and confectionary industries to reduce the cost on importation of the conventional baker's yeasts.

ACKNOWLEDGEMENT

My profound gratitude goes to the Tertiary Education Trust Fund (TETFUND) for creating and funding the Institution Based Research (IBR) Grant which granted the opportunity and funding of this research work.

I also appreciate the management of Nnamdi Azikiwe University, for the effort in processing my Proposal which gave me the opportunity to access and perform this work. To all those who helped in one way or the other to achieve this goal, I say thank you all.

REFERENCES

- [1] Agwuna L.C., Umeh S.O. and Egbuim T.C. (2019). Study o the wine production attributes of *Saccharomyces cerevisiae* isolated from sucrose enriched palm wine and non-sucrose enriched palm wine. *Int. Journal of Agric and Biosciences*. **8** (5): 256-258.
- [2] Benitez, B., Gasent, R. J. M., Castrejon, F. and Codon, C. (1996) Development of new strains for the food industry. *Journal of Biotechnology* **12**: 149–163.
- [3] Casas-Godoy L., Arellano-Plaza M., Kirchmayr M., Barrera-Martinez I and Gschaedler- Mathis A. (2021). Preservation of non-Saccharomyces yeasts: current technologies and challenges. *Comprehensive reviews in food science and food safety*. **20** (4):3464- 3503.
- [4] Cavalieri, D., Townsend, J., Polsinelli, M. and Hartl, D. (2001) Whole genome expression analysis of colony morphology in vineyard isolates of *Saccharomyces cerevisiae*. *Yeast Review* **18**: 110-112.
- [5] Chilaka C.A., Uchekukwu N. and Akpor O.B. (2010). Evaluation of the efficiency of yeast isolates from palm wine in diverse fruit wine production. *African Journal of Food Science* **4** (12): 762-774.
- [6] Chi Z. and Ameborg N. (2000). *Saccharomyces cerevisiae* strains with different degrees of ethanol tolerance exhibit different adaptive responses to produced ethanol. *Journal of Industrial Microbiology and Biotechnology* **24**: 75-78.
- [7] Chiranjeev T., Hari P.O., Nanda K.Y. and Matcha B. (2013). Isolation and characterization of ethanol tolerant yeast strains. *Journal of Bioinformatics* **9** (8): 421-425.
- [8] Fleury, R. Y., Bel, R. R. and Juillerat, M. A. (2002) Enzyme. *Journal of Molecular Catalysis* **20**: 473-477.
- [9] Graham, H. Fleet (2007). Yeast in foods and beverages: impact on product quality and safety. *Current Opinion in Biotechnology*, **18**: 170-175.
- [10] Iraj, N. Giti, E., and Lila, A. (2002) Isolation of a flocculation of *Saccharomyces cerevisiae* and investigation of its performance in the fermentation of beet molasses to ethanol. *American Journal of Biomass and Bioenergy* **23**: 481-486.
- [11] Irena V., Marta H., Blanka J. and Zdena P. (2005). The Morphology of *Saccharomyces cerevisiae* colonies affected by cell adhesion and the budding pattern. *Research in Microbiology*, **156**: 921-930.
- [12] Kevin, K. (2005). Fungi: Biology and Applications. England: John Wiley and Sons, Ltd. p 257.
- [13] Kurtzman, C.P., and Fell, J.W.(1998) The Yeast, a taxonomic study 4th edition. Elsevier Science Publisher, Amsterdam.pp77-121.

- [14] Kuthan M., Devaux F., Janderova B. Slaninova I., Jacq C. and Palkova Z. (2003). Domestication of wild *Saccharomyces cerevisiae* accompanied by changes in Gene expression and colony Morphology. *Molecular Microbiology* **47**: 745-754.
- [15] Martini, A. (1993) Origin and domestication of the winery yeast *Saccharomyces cerevisiae*. *Journal of wine Research* **4**: 165-176
- [16] Mortimer, R. K. (2000) Evolution and variation of yeast (*Saccharomyces*) genome. *Genome Research* **10**: 403-409.
- [17] Sergi, M. (2020). The role of yeasts in fermentation processes. *Microorganisms* **8** (8):1142 DOI:10.3390/microorganisms 8081142.
- [18] Tarek, M. E-N. (2001) Immobilization of recombinant strains of *Saccharomyces cerevisiae* for the hydrolysis of lactose in salted Domiati cheese whey. *European Food Research and Technology* **212**: 225-227.
- [19] Thais, M., Danilo G. and Tania, M.B. (2006) Isolation and characterization of *Saccharomyces cerevisiae* strains of winery interest. *Brazilian Journal of Pharmaceutical Sciences*.**42**:119-126.
- [20] Umeh, S.O., Agwuna, L.C. and Okafor U.C. (2017): Yeast from local sources: An alternative to the conventional Brewer's yeast. *World Journal of Multidisciplinary Research and Development* **3** (10) 191-195.
- [21] Umeh, S.O. and Okafor, J.N.C. (2016): Isolation, Characterization and Identification of Yeast (*Saccharomyces cerevisiae*) from Three Local Beverage Drinks. *International Journal Series in Multidisciplinary Research* **2** (5) 44 – 55.
- [22] Umeh, S.O., Okpalla, J. and Okafor, J.N.C. (2019): Novel Sources of *Saccharomyces* Species as Leavening Agent in Bread Making. *International Journal of Trend in Scientific Research and Development (IJTSRD)*, **3** (2) 827-832.
- [23] Umeh, S.O., Udemezue, O., Okeke, B.C. and Agu., G.C. (2015). Pawpaw (*Carica papaya*) wine: with low sugar produced using *Saccharomyces cerevisiae* isolated from a local drink 'Burukutu'. *International Journal of Biotechnology and Food Science*, **3** (2): 17-22.
- [24] Yabaya, A. and Jatau, E.D. (2009). Investigating wild yeast baking potentials. *Middle East Journal of Scientific Research*. **4** (4): 320-322.

Indoor Environment of Buildings – Quality and Basic Ventilation Air Parameters: Part I

Lubomira Kmetova¹, Romana Dobakova², Lukas Toth³

Department of Power Engineering, Faculty of Mechanical Engineering, Technical University of Košice, Slovakia

Received: 01 October 2022/ Revised: 13 October 2022/ Accepted: 18 October 2022/ Published: 31-10-2022

Copyright © 2021 International Journal of Engineering Research and Science

This is an Open-Access article distributed under the terms of the Creative Commons Attribution Non-Commercial License (<https://creativecommons.org/licenses/by-nc/4.0>) which permits unrestricted Non-commercial use, distribution, and reproduction in any medium, provided the original work is properly cited.

Abstract— A series of articles focused on the indoor environment of buildings. Articles discuss the importance of a quality indoor environment and the implementation of the measurement of the parameters of the outgoing air from the indoor environment in the ventilation shaft of an apartment building. The content of the first article is a description of pathogens disrupting the indoor environment, manifestations of sick building syndrome, the need for ventilation.

Keywords— *Indoor Environment, Sick Building Syndrome, Ventilation Shaft.*

I. INTRODUCTION

Air is irreplaceable for breathing of all living organisms. Millions of citizens within the WHO European Region spend approximately 90% of their time indoors: in their homes (2/3 of this time), workplaces, schools, and public spaces. In recent years, the covid 19 pan-demic, high workload, and ongoing climate change have had an impact on increasing the amount of time people spend indoors to this level. And that is why the quality of this internal environment is very important, on which our health, satisfaction, well-being, but also productivity and performance depend. [1, 2]

Indoor air can be defined as air that has an indirect connection with outdoor air and is so influenced by indoor sources and activities that its quality can differ significantly from outdoor free air. [3]

II. POLLUTANTS OF THE INDOOR ENVIRONMENT

Pollutants of the indoor environment of buildings can be divided into the three following groups [3]:

- Chemical pollutants,
- Fine dust particles,
- Biological pollutants.

To identify and solve problems, pollutants can also be divided into [3, 4]:

- Pollutants, the source of which is building material and furniture, in particular: volatile organic compounds (VOC), asbestos, formaldehyde, dust particles,
- Pollutants, the source of which is human activity, in particular: VOC, CO, pesticides, tobacco smoking - ammonia, nicotine, nitrosamine, benzo-a-pyrene,
- Pollutants produced during combustion, in particular: CO, NO₂, VOC, dust particles,
- Outdoor air pollutants, in particular: CO, NO₂, VOC, dust particles, ozone,
- Pollutants arising in connection with the occurrence of moisture in buildings - moulds, mites, microorganisms, and VOC.

III. SICK BUILDING SYNDROME

A significant amount of energy is required to create thermal, light, or acoustic comfort, or to ensure high-quality, hygienically required indoor air without the presence of hazardous substances, which is used by environmental engineering systems, especially in public and residential buildings. [3]

The negative impact of various factors of the internal living environment on human health can lead to various health problems, such as allergic or infectious diseases. Triggers of these health problems are chemicals, viruses, bacteria, or moulds found in the indoor environment of buildings. These problems can be generally divided into two categories [5, 6]:

- Sick Building Syndrome (SBS),
- Building-Related Illnesses (BRI).

Manifestations of SBS are non-specific and tend to be associated with many factors, including temperature and humidity extremes in the environment. SBS is mainly manifested by itching and watery eyes, irritation and stuffy nose, throat irritation, coughing, choking, hoarseness. There is also skin irritation (allergies, itching, dry skin), hair loss, headaches, exhaustion, fatigue, reduced mental capacity, changes in sensitivity to smell, and taste, etc. [5, 6].

Confirmation of the negative health effects of the indoor environment on our health requires the use of standardized, accurate and objective methods of monitoring the relationship between the indoor microclimate (temperature, relative humidity, dustiness, air exchange, used construction materials and equipment of buildings, their external environment) and microorganisms (e.g. moulds). [5, 6].

The high occurrence of microorganisms in the indoor environment is caused both by insufficient heating of living spaces (i.e., the occurrence of temperatures below 20 °C in the indoor environment) and high relative humidity (i.e. above 50% for a long time). [7].

Regular air exchange (ventilation) plays a very important role in creating a high-quality indoor environment, especially for maintaining optimal air humidity. Ventilation, whether natural or managed (using the environmental engineering systems) is necessary for [7]:

- Fresh air supply,
- Maintaining a healthy relative humidity,
- Maintaining a low CO₂ level.

IV. VENTILATION

Ventilation moves outdoor air into a building or a room and distributes the air within the building or room. The general purpose of ventilation in buildings is to provide healthy air for breathing by both diluting the pollutants originating in the building and removing the pollutants from it [8, 9]. During ventilation, there is no adjustment of the air properties, the adjustment of the air properties is provided by the air conditioning, for example, the adjustment of the air temperature. [10]

Building ventilation has three basic elements [11]:

- Ventilation rate — the amount of outdoor air that is provided into the space, and the quality of the outdoor air,
- Airflow direction — the overall airflow direction in a building, which should be from clean zones to dirty zones,

- Air distribution or airflow pattern — the external air should be delivered to each part of the space in an efficient manner and the airborne pollutants generated in each part of the space should also be removed in an efficient manner.

There are three methods that may be used to ventilate a building: natural, mechanical and hybrid (mixed mode) ventilation.

Areas prone to the formation of moulds are:

- Unventilated or improperly ventilated rooms (e.g., continuously cooled spaces due to the opening of ventilation holes),
- Hypothermic rooms (also in connection with saving on heating),
- Rooms with windows without micro-ventilation systems,
- Inappropriately insulated rooms (e.g., internal insulation).

This subsequently leads to a deterioration in the quality of the living space not only in terms of aesthetics (unwanted growths of fungi on interior walls, furniture, upholstery, etc.), but above all in terms of health.

Special attention should be paid to the air conditioning system, especially if it includes air humidifiers. The fact that we neglect the regular maintenance of filters, and all air conditioning systems leads to a significant increase in the concentration of germs of microorganisms in the air compared to untreated air (up to a 10,000-fold increase in the number of fungal germs in 1 m³ of air is reported). [6]

Several European standards are devoted to the ventilation of buildings, for example: EN 1886:2007 Ventilation for buildings. Air handling units. Mechanical performance; EN 12599:2012 Ventilation for buildings – Test procedures and measurement methods to hand over air conditioning and ventilation systems; EN 13053:2019 Ventilation for buildings – Air handling units – Rating and performance for units, components and sections; EN 13141 Ventilation for buildings – Performance testing of components/products for residential ventilation – Part 1 to Part 10; CEN/TR 16798 Energy performance of buildings – Ventilation for buildings – Part 1 to Part 18.

V. ORIGINAL CONDITION OF VENTILATION IN APARTMENT BUILDINGS

Ventilation in the original construction was based on leaking windows (Fig. 1). Their normal leakage ensured the necessary and permanent exchange of air. At present, the insulation or renovation of apartment buildings is widely used. The owners are thus trying to save heating costs.

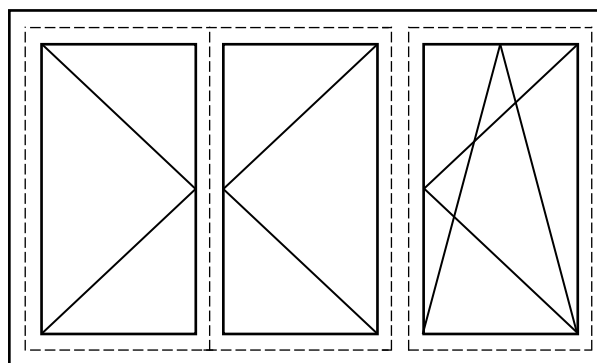


FIGURE 1: Scheme of the window with marking of ventilation gap [12]

If the building is thoroughly sealed without an alternative increase in air flow, the indoor climate will deteriorate, while the concentration of harmful substances (CO₂) and humidity will increase. There is a risk of mould formation in the living space [12].

Ventilation systems in mass housing construction were part of separately produced housing cores and installation shafts. The oldest panel houses in Slovakia have a built-in air duct in the installation shafts. Horizontal connections from the bathroom, toilet, and kitchen lead to this duct. The vent duct cap was usually installed on the outlet of the air duct on the roof of the panel house (Fig. 2).



FIGURE 2: The vent duct cap [13]

VI. METHODOLOGY FOR MEASURING THE AMOUNT AND PARAMETERS OF VENTILATION AIR

The measurement of ventilation air parameters needs to be taken comprehensively. It is important to have:

- A theoretical basis for ventilation air parameters,
- Then prepare the measurement,
- Perform the measurement itself,
- Evaluate the measurement.

VII. THEORY OF VENTILATION AIR PARAMETERS

Moist or humid air is a mixture of dry air and water vapour. The state of the air is defined by two quantities - temperature and humidity. Processes that work with moist air are mostly isobaric. This means that the corresponding pressure in the air duct differs very little from the atmospheric pressure [14, 15].

For calculations of thermal processes of moist air are applied [15]:

- Dalton's Law,
- Gas equation of state.

The relative humidity (φ or RH) is the ratio (as percentage) of the partial pressure of water vapor in air, to the vapor pressure of liquid water at the same temperature [16].

VIII. CONCLUSION

The quality of the internal environment of buildings is a topic that needs to be addressed now, especially in view of the still persistent increased risk of the spread of the Covid-19 virus and other respiratory diseases. There are also other threats to our health in connection with the prolonged exposure of humans in the internal, working or living environment of buildings. The quality of the internal environment needs to be addressed with the same importance even in view of the ongoing climate crisis. We need to deal more and more intensively with the transition from the use of fossil fuels to sustainable energy sources. And to the possibilities of how to minimize heat losses, for example by ventilation, but on the other hand, so that the internal microclimate is not affected by this. This means that it is necessary to maintain hygienic air exchange in the indoor environment. Before starting the measurement of the quality of the internal environment of the living space (more in the article Indoor Environment of Buildings – Quality and Basic Ventilation Air Parameters, Part II.) from the energy point of view, it was desirable to define this issue from a theoretical point of view, which was the content of this article.

ACKNOWLEDGEMENTS

This paper was written with the financial support from the VEGA granting agency within the project solutions No. 1/0626/20 and No. 1/0532/22 from the KEGA granting agency within the project solutions No. 012TUKE-4/2022 and with financial

support from the granting agency APVV within the Project Solution No. APVV-15-0202, APVV-21-0274 and APVV-20-0205.

REFERENCES

- [1] Management of Emerging Public Health Issues and Risks. Multidisciplinary Approaches to the Changing Environment. Elsevier, 2019. Pages 314. ISBN 978-0-12-813290-6.
- [2] WHO Regional Office for Europe. Combined or multiple exposure to health stressors in indoor built environments. 2014. Pages 80. <https://www.euro.who.int/__data/assets/pdf_file/0020/248600/Combined-or-multiple-exposure-to-health-stressors-in-indoor-built-environments.pdf>. (accessed 20.09.2022)
- [3] National reference centre for the evaluation of the impact of free air and the air of non-production indoor spaces on population health. Factors of the indoor air of buildings and their impact on the health of residents. 2010. Pages 18. <https://www.vzbb.sk/sk/urad/narodne_centra/nrc_vo/factory_vnut_ovzdušia101001.pdf>. (accessed 20.09.2022)
- [4] Vardoulakis, S. et al. Impact of climate change on the domestic indoor environment and associated health risks in the UK. In: Environment International, Volume 85, 2015. Pages 299-313. ISSN 0160-4120.
- [5] Encyclopedia of Toxicology. 3rd Edition. Academic Press 2014. Pages 256 – 260. ISBN 978-0-12-386455-0.
- [6] Survey: Is there Good Quality of the Indoor Environment in the Buildings? In: TZB HAUSTECHNIK, Volume: 23 (02), 2015. Pages 40 – 43.
- [7] WHO guidelines for indoor air quality: dampness and mould. 2009. Pages 248, ISBN 978-92-890-4168-3.
- [8] Etheridge D, Sandberg M. Building ventilation: Theory and Measurement. Chichester, UK: John Wiley & Sons; 1996. Pages 754. ISBN 978-0471960874.
- [9] Awbi HB. Ventilation of buildings. 2nd Edition. New York: Taylor & Francis; 2003. Pages 522. ISBN 0-203-63447-0.
- [10] Dufka, J. Ventilation and air conditioning of houses and flats. 2nd Edition. Prague: Grada Publishing, 2005. Pages 128. ISBN 80-247-1144-3.
- [11] WHO. Natural Ventilation for Infection Control in Health-Care Settings. Geneva, 2009. Pages 106. ISBN 978-92-4-154785-7.
- [12] Kapalo, P. Reconstruction of the ventilation system in an apartment building – part 1. In: Plynár – Vodár – Kurenár + Klimatizácia, Volume 2/2010. p. 34 – 36. ISSN 1335-9614.
- [13] Figure 2.: The vent duct cap. [online]. <<https://www.iventilatory.sk/ochranna-kovova-hlavica-pre-zakoncenie-vzduchoveho-rozvodu-200mm.html>>. (accessed 20.09.2022)
- [14] Pauline M. Doran. Bioprocess Engineering Principles. 2nd Edition. Elsevier, 2013. Chapter 11. Pages 445-595. ISBN 978-0-12-220851-5.
- [15] Széknyová, M. et al. Technical equipment of buildings III. 1st Edition. Bratislava: Publishing house of the Slovak Technical University, 2001. 272 s. ISBN 80-227-1590-5.
- [16] Berk, Z. Food Process Engineering and Technology. Elsevier, 2009. Chapter 22. Pages 459-510. ISBN 978-0-12-373660-4.

Comparison of Different Natural Gas Flow Rates in Pipelines and their Effect on Odorant Concentration

Ivan Mihalik^{1*}, Tomas Brestovic², Romana Dobakova³, Lukas Toth⁴

Department of Power Engineering, Faculty of Mechanical Engineering, Technical University of Košice, Slovakia

*Corresponding Author

Received: 01 October 2022/ Revised: 15 October 2022/ Accepted: 22 October 2022/ Published: 31-10-2022

Copyright © 2021 International Journal of Engineering Research and Science

This is an Open-Access article distributed under the terms of the Creative Commons Attribution Non-Commercial License (<https://creativecommons.org/licenses/by-nc/4.0>) which permits unrestricted Non-commercial use, distribution, and reproduction in any medium, provided the original work is properly cited.

Abstract— The article deals with the problem of adding and spreading an odorant in a high-pressure pipeline. Briefly describes the basic properties of odorants added to natural gas. Furthermore, it mainly focuses on the odorant concentration in natural gas at different natural gas flow rates. By using the ANSYS CFX software, simulations were carried out on the pipeline models representing the selected section of the distribution network at the maximum, minimum and zero flow of natural gas.

Keywords— CFD Simulation, High-Pressure Pipeline, Odorization Techniques, Natural Gas.

I. INTRODUCTION

Natural gas is a mixture of gaseous hydrocarbons. Among its main components is mainly methane, which makes up approximately 93% to 99% of its content. In addition, natural gas also contains propane, butane and other substances. Natural gas serves mainly as a natural fuel for heating and DHW, further for cooking, or in the form of CNG as a fuel for cars. Among its advantages are good controllability and distribution, there is also no need to provide storage space for the customer.

Natural gas is lighter than air, it is flammable, colorless, tasteless and has no natural smell. Although it is not a poisonous gas, it is non-breathable. It is the absence of odor that appears to be problematic from the safety point of view. For this reason, natural gas odorization is necessary. The importance of odorization lies in the early warning of people in the event of an accidental gas leak either from a gas pipeline or from a delivery point. Thanks to early detection of a natural gas leak, an explosion, fire or suffocation can be prevented.

II. ODORANTS PROPERTIES

An odorant is defined as a characteristically odorous substance added to other odorless, usually hazardous substances in order to signal their presence. The role of odorants is to ensure gas leak detection without the need to use any equipment. The end user must be able to detect a possible leak with his own sense of smell. Odorants therefore enable the detection of gas leaks even in places where the placement of special detectors would be complicated or completely impossible.

The ideal odorant should be an easily recognizable specific odor with a strong enough intensity that the use of a low concentration of the odorant in the gas is sufficient. The odorant used in natural gas should have a good ability to penetrate the ground so that in the event of a pipeline breach in the ground and a subsequent leak, it can warn people on the surface. At the same time, however, it cannot penetrate through an intact pipeline, nor can it disturb it by its own action. It must also not change the physical and chemical properties of natural gas, except for adding an odor.

There are two basic groups of odorants, namely sulfur-based and sulfur-free odorants. Sulfur-based odorants are traditional odorants. This group includes, for example, mercaptans, sulfides and sulfur-containing heterocycles. Mercaptans, also called thiols with the formula R-SH, are sulfur analogs of alcohols and phenols. They react similarly but are more acidic. They are insoluble in water, but they are soluble in ethanol or diethyl ether. They cause a very strong, pervasive and unpleasant smell. Instead of an oxygen atom, their molecules contain a sulfur atom. The functional group of mercaptans is -SH. Mercaptans are mostly liquid substances, except for methanethiol, which is in gaseous form. These types of odorants are also commonly found in the wild nature. In practice, however, various mixtures of several types of odorants are currently used to take full advantage of their positive properties. In this way, the optimal properties of the odorant can be achieved.

III. PIPELINE MODEL IN THE EXAMINED SECTION

The model of the pipeline section was created using CAD software PTC Creo. The simulation of the natural gas and odorant mixture spreading in the investigated section was subsequently carried out in the ANSYS CFX software. The examined pipe section is shown in Fig. 1 when viewed from above.

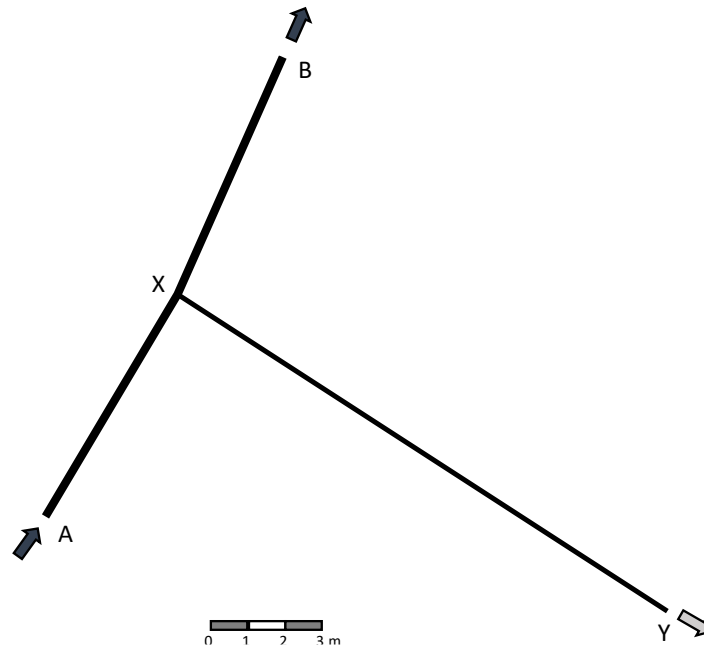


FIGURE 1: The examined section of the distribution network

The section between points A and B represents the main pipe with a diameter of $D = 200$ mm, while natural gas enters point A. A secondary pipe with a diameter of $D = 80$ mm is connected to the main pipe at point X. Due to the negligible value of elevation on the selected section of the main pipeline, and no elevation of the secondary pipe, it is possible to consider this section of the pipe network as horizontal. The distances between individual points of the section are defined in Table 1.

**TABLE 1
PIPE LENGTH OF SELECTED SECTIONS**

Section	Length (m)
A – X	7
X – B	7
X – Y	16

Due to the low partial pressure of the odorant in the pipeline, it can be assumed that the odorant added to natural gas in liquid form always evaporates even at high operating pressures and normal temperatures. This statement is also confirmed by long-term observation of the behavior of odorants added to natural gas in practice. Thus, a homogeneous mixture of natural gas and odorant occurs in the pipeline.

IV. ODORANT CONCENTRATION AT THE DELIVERY POINT AT MAXIMUM FLOW

Before the simulation, it was necessary to set the boundary conditions. At the time of maximum flow through the main pipeline, $Q_{mA1} = 0.1034$ kg·s⁻¹ of natural gas entered point A of pipeline. At delivery point Y, the amount of taken gas was $Q_{mY1} = 0.0036$ kg·s⁻¹. As the natural gas in the main pipe flowed further from point B, it was necessary to define the relative pressure $p_{rel} = 0$ Pa at this point. The pressure at point A at maximum flow is $p_{A1} = 3.164$ MPa. Odorant volume fraction $\phi_{THT} = 1.0447 \cdot 10^{-5}$. The gravitational acceleration $g = 9.81$ m·s⁻² was also considered.

In addition to boundary conditions, it was also necessary to define the material properties of natural gas and odorant. The molar mass of natural gas was calculated according to its current composition. Its density and dynamic viscosity were defined using the .ccl file as a function for temperatures in the range 0-20 °C and pressures in the range 2-4 MPa. This file was subsequently

imported into the ANSYS program. The molar mass and dynamic viscosity of the odorant was read from the safety data sheet. Odorant density was defined as a function using equation (1) derived from the equation of state:

$$\rho_{THT} = \frac{p_{THT} \cdot M_{THT}}{R \cdot T} \tag{1}$$

where p_{THT} is the partial pressure of the odorant (Pa), M_{THT} – molar mass of the odorant ($\text{kg} \cdot \text{mol}^{-1}$), R – universal gas constant ($8314 \text{ J} \cdot \text{kmol}^{-1} \cdot \text{K}^{-1}$), T – thermodynamic temperature (K).

The simulation results show in Fig. 2 the natural gas flow velocity and in Fig. 3 the odorant volume fraction when viewed from above on the XY plane in the pipeline axis at maximum flow:

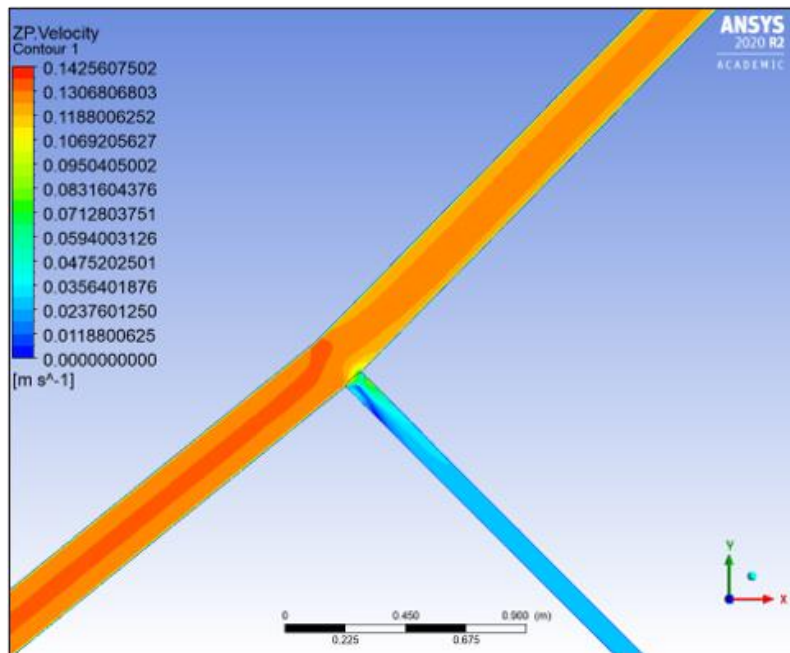


FIGURE 2: Natural gas velocity at max. flow rate

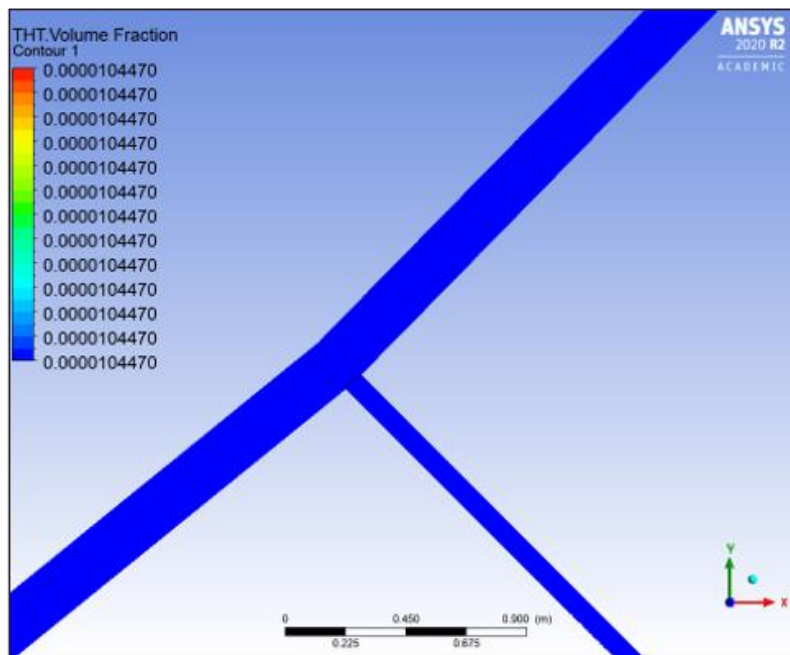


FIGURE 3: Odorant volume fraction at max. flow rate

The result shows that at the maximum flow rate of natural gas, there is no change in the concentration of the odorant in the pipeline along its length in the axis of the pipeline. Using the AreaAve function in the ANSYS program, it was also verified that the concentration does not change even in the cross-section of the pipe at the delivery point Y.

V. ODORANT CONCENTRATION AT THE DELIVERY POINT AT MINIMUM FLOW

At the minimum flow rate at point A in the main pipe $Q_{mA2} = 0.0038 \text{ kg}\cdot\text{s}^{-1}$, the pressure at this point of the pipe was $p_{A2} = 3.179 \text{ MPa}$. The flow rate at delivery point Y was $Q_{mY2} = 0.0007 \text{ kg}\cdot\text{s}^{-1}$. The volume fraction and material properties were defined as in the simulation at maximum flow. The results of the simulation show in Fig. 4 natural gas velocity and in Fig. 5 volume fraction of the odorant when viewed from above on the XY plane in the pipe axis at minimum flow rate:

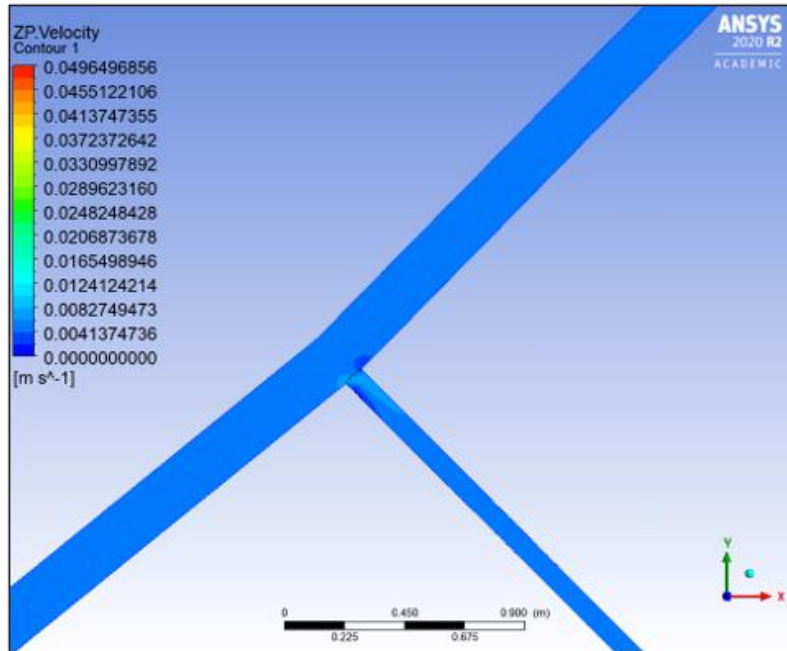


FIGURE 4: Natural gas velocity at min. flow rate

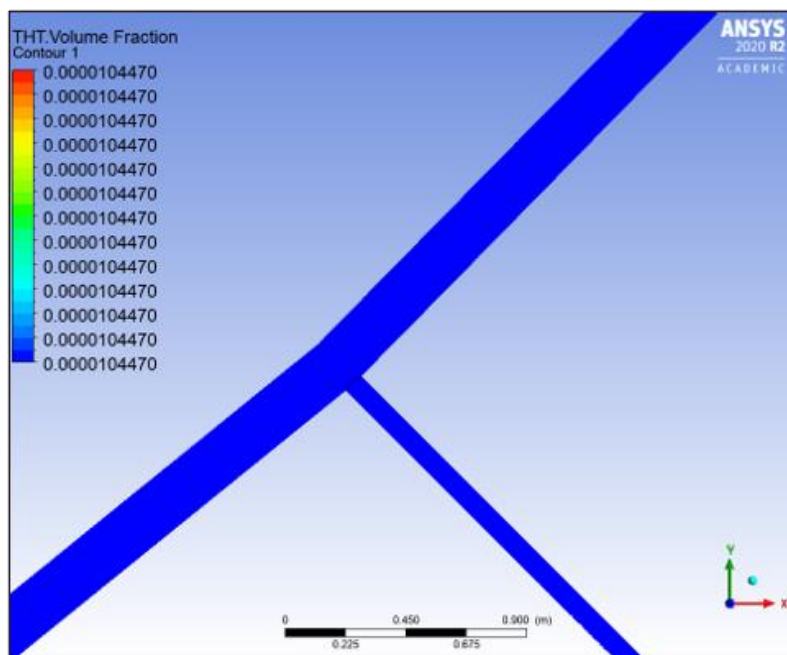


FIGURE 5: Odorant volume fraction at min. flow rate

As in the previous simulation, even in the case of minimum flow, there is no change in the odorant concentration in the natural gas in the axis of the pipe, nor in its cross-section at the delivery point.

VI. ODORANT CONCENTRATION AT THE DELIVERY POINT AT ZERO CONSUMPTION AND MAXIMUM FLOW RATE IN THE MAIN PIPELINE

In this simulation, the goal was to verify a possible change in concentration in an extreme theoretical situation, when at the maximum flow of natural gas in the main pipeline, a state of zero consumption would occur at the delivery point Y. The flow rate and pressure at point A were the same as in the first simulation, the flow rate in delivery point Y was $Q_{mY3} = 0 \text{ kg}\cdot\text{s}^{-1}$. The other parameters remained same as in the previous simulations.

Fig. 6 shows the velocity of natural gas and Fig. 7 shows the odorant volume fraction at zero consumption.

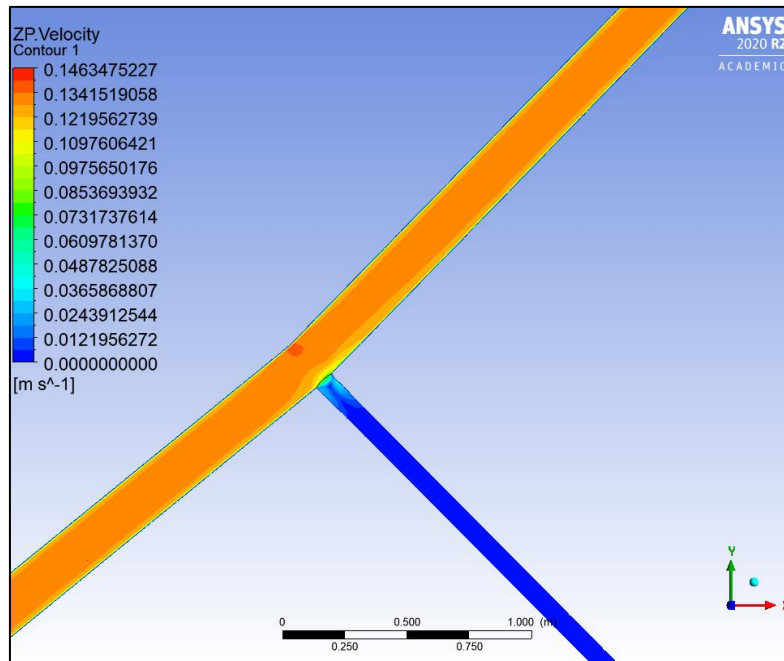


FIGURE 6: Natural gas flow rate at max. flow rate and zero consumption

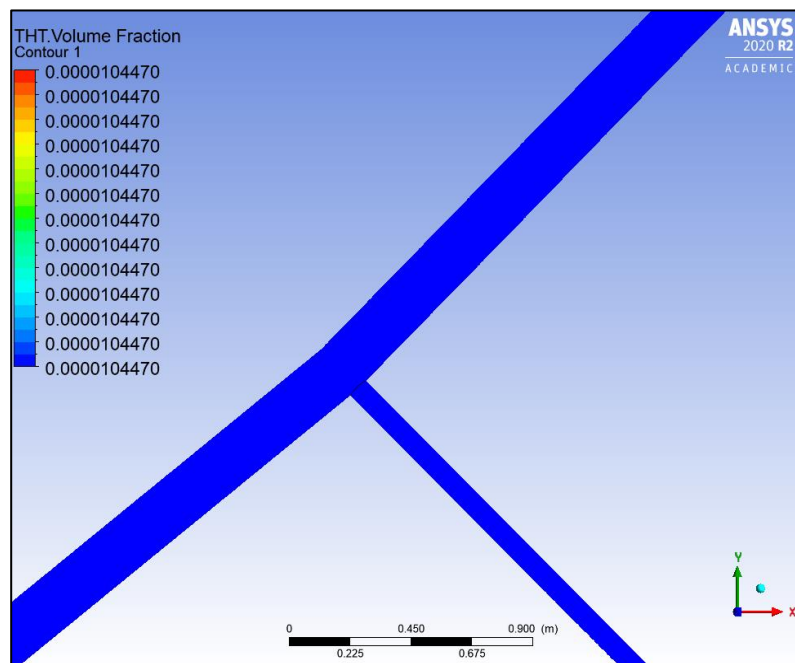


FIGURE 7: Odorant volume fraction at max. flow rate and zero consumption

As can be seen from the results, even in this extreme situation there was no change in the concentration of the odorant in the natural gas.

VII. CONCLUSION

Describing the behavior of an odorant in natural gas is quite complicated, since in addition to physical processes, it is also affected by chemical processes such as adsorption, absorption and oxidation. As a result of these processes, the odorant concentration in natural gas may decrease after a certain period of time. In this article, the focus was on the actual flow of the mixture of odorant and natural gas without the influence of chemical processes. The simulations confirmed the assumption that after the vaporization of the odorant in the pipe, an unchanging homogeneous mixture is formed, regardless of the gas flow rate in the pipeline.

ACKNOWLEDGEMENTS

This paper was written with the financial support from the VEGA granting agency within the project solutions No. 1/0626/20 and No. 1/0532/22 from the KEGA granting agency within the project solutions No. 012TUKE-4/2022 and with financial support from the granting agency APVV within the Project Solution No. APVV-15-0202, APVV-21-0274 and APVV-20-0205.

REFERENCES

- [1] MOULI-CASTILLO, J. et al. 2021. A comparative study of odorants for gas escape detection of natural gas and hydrogen. In: *International Journal of Hydrogen Energy*, 2021, Vol. 46., p. 14881-14893.
- [2] J. FINK, J. 2015. Chapter 15 – Odourisation. In: *Petroleum Engineer's Guide to Oil Field Chemicals and Fluids*, 2015, p. 455–475.
- [3] KILGALLON, R. 2015. Odourisation of CO₂ pipelines in the UK: Historical and current impacts of smell during gas transport. In: *International Journal of Greenhouse Gas Control*, 2015, Vol. 37., p. 504–512.
- [4] TENKRAT, D., HLINCIK, T., PROKES, O. 2010. Chapter 4 – Natural Gas Odorization. In: *Natural Gas*, 2010, p. 87–103.
- [5] BRESTOVIČ, T. – JASMINSKÁ, N. 2015. *Numerické metódy a modelovanie v energetike*. 1. vyd. Košice: Technická univerzita v Košiciach, Strojnícka fakulta, 2015. 113 s. ISBN 978–80–553-2067-0.



AD Publications

**Sector-3, MP Nagar, Bikaner,
Rajasthan, India**

www.adpublications.org, info@adpublications.org